



GT-2 Magnetometry: an introduction

P. Vavassori

-Ikerbasque, Basque Foundation for Science and CIC nanoGUNE Consolider, San Sebastian, Spain.





Introduction -Outline

This lecture will provide an introduction to a number of important tools and methods employed in the investigation of magnetic materials.

They will focus on magnetometry tools and approaches available in most laboratories:

- magneto-optical Kerr effect (MOKE) magnetometry.**
- vibrating sample magnetometry (VSM),**
- superconducting quantum interference device (SQUID),**
- torque magnetometry,**
- alternating gradient magnetometry,**

Consideration will be also given to the special problems posed by measurements on feebly magnetic materials, like nanostructured ones, basic requirements regarding sensitivity and accuracy, and potential artifacts.



Magnetometry: what we would like to measure?

- **Saturation magnetization**
- **Remnant magnetization**
- **Coercive field**
- **Switching field**
- **Anisotropy symmetry and energy**
- **Reversal process**

.....

At the nanoscale



Units



$$\oint_S \vec{H} d\vec{s} = \iint_A \vec{j} d\vec{A}$$

(Ampère's law)

$$H = \frac{I}{2\pi r} \left[\frac{\text{A}}{\text{m}} \right]$$

what about Tesla [T]? $\text{rot } \vec{B} = \mu_0 \vec{j}$

B [T]: magnetic induction
 $\mu_0 = 4\pi \cdot 10^{-7} [\text{T m / A}]$
permeability of free space

$$B = \frac{\mu_0 I}{2\pi r} \quad [\text{T}]$$

and Oersted [Oe]? $1 \text{ T} = 10^4 \text{ Oe} = 0.796 \frac{\text{MA}}{\text{m}}$

1 T is a large field..., 100 A in 1 cm: ONLY 2mT



Constitutive equations and units

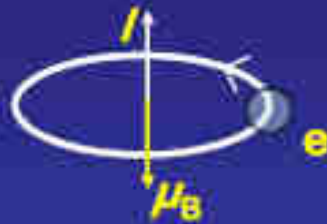
Magnetization \vec{M} and magnetic moment \vec{m}

$$\vec{B} = \mu_0 (\vec{H} + \vec{M}) \quad \text{Sommerfeld convention}$$

$$\vec{M} = \frac{N}{V} \vec{m}$$

total magnetic moment per volume,
N: number of magnetic moments
V: volume

atomic magnetic moment: Bohr magneton μ_B



classical picture
-WRONG-

$$\mu_B = \frac{e \hbar}{2 m_e} = 9.274 \times 10^{-24} \text{ A m}^2 \quad [\text{J/T}]$$

1 μ_B : magnetic moment of 1 electron spin

$$(1 \text{ emu} = 10^{20} \mu_B = 10^{-3} \text{ Am}^2)$$



Summary constitutive equations and units

$$\mathbf{M} = \chi_m \mathbf{H}$$

$$\mathbf{B} = \mu_0(\mathbf{H} + \mathbf{M}) \rightarrow \mathbf{B} = \mu\mathbf{H}$$

$$\mu = \mu_0(1 + \chi_m)$$

Cgs System

$$\mathbf{B} = (\mathbf{H} + 4\pi \mathbf{M}) \quad \mu_0 = 1$$

$$\mu = (1 + 4\pi \chi_m)$$

cgs

SI

H units Oe A/m

B units Oe T

M units emu /cm³ A/m

Conversions:

For **H** 1Oe = 10³/ 4π A/m = 79,58 A/m

For **B** 1T = 10⁴Oe

For **M** 1emu/cm³ = 10³ A/m

Magnetic moment 1 Am² = 10³ emu

$$1 \text{ emu} = 10^{20} \mu_B = 10^{-3} \text{ Am}^2$$

$$1 \mu_B = 9.274 \cdot 10^{-24} \text{ Am}^2 \text{ [J/T]}$$



Basics: diamagnetism and paramagnetism

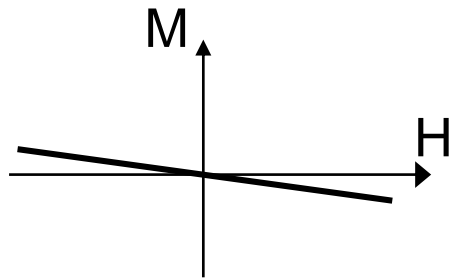
Every material which is put in a magnetic field \mathbf{H} , acquires a magnetic moment.

In most materials $\mathbf{M} = \chi_m \mathbf{H}$ (\mathbf{M} magnetic dipole per unit volume, χ magnetic susceptibility).

$$\boldsymbol{\mu} = -\mu_B(\mathbf{L} + g\mathbf{S})$$
 orbital and spin angular momenta

$$\text{In solids } \boldsymbol{\mu} \approx -g\mu_B \mathbf{S} \text{ (crystal field)}$$

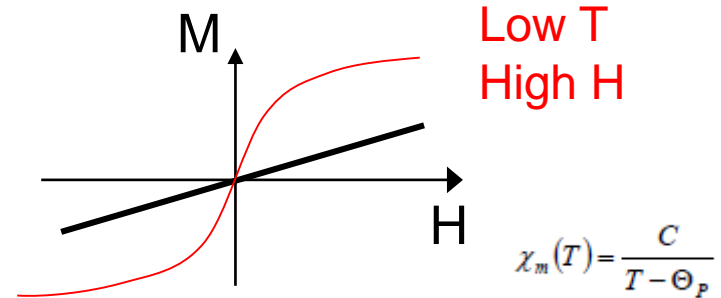
diamagnetism



Each atom acquires a moment caused by the applied field \mathbf{H} and opposed to it (Larmor frequency).

$$\boldsymbol{\mu} = 0 \text{ e.g., noble gas.}$$

paramagnetism



Each atom has a non-zero magnetic moment $\boldsymbol{\mu}$; The moments are randomly oriented (T); \mathbf{H} arranges these moments in its own direction.

$$E_{\text{appl}} = -\mu_0 \mathbf{M} \cdot \mathbf{H} \longleftrightarrow \text{temperature } k_B T$$



Ferromagnetism

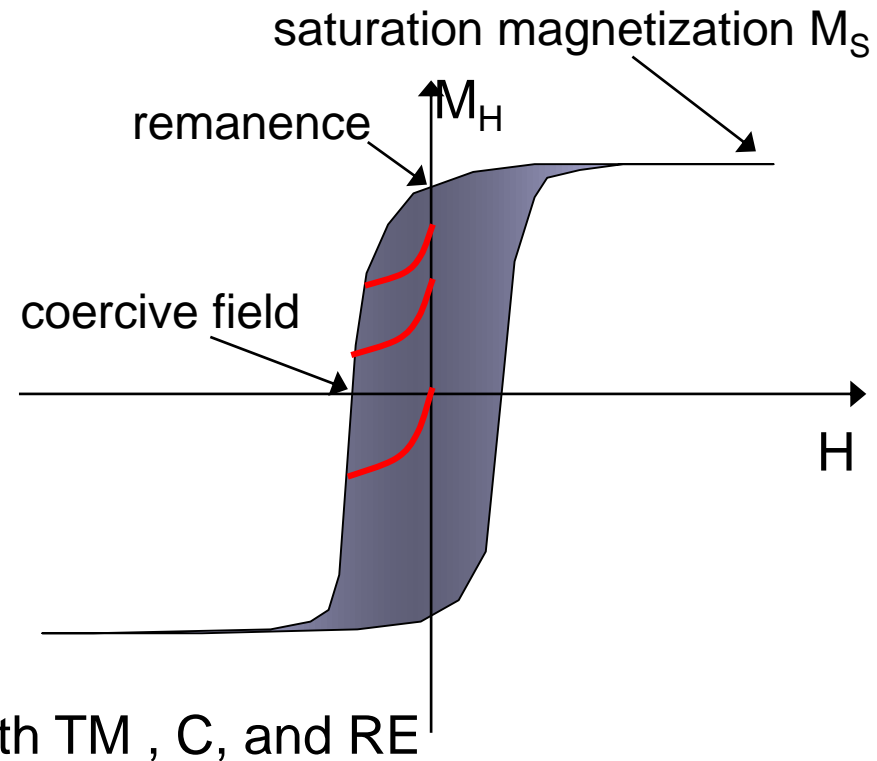
There are materials in which \mathbf{M} is NOT proportional to \mathbf{H} .

\mathbf{M} may be, for example, non-zero at $\mathbf{H} = 0$.

\mathbf{M} in these materials is not even a one-valued function of \mathbf{H} , and its value depends on the history of the applied field (hysteresis).

Limiting hysteresis curve: all the points enclosed in the loop are possible equilibrium states of the system.

With an appropriate history of the applied field one can therefore end at any point inside the limiting hysteresis loop.

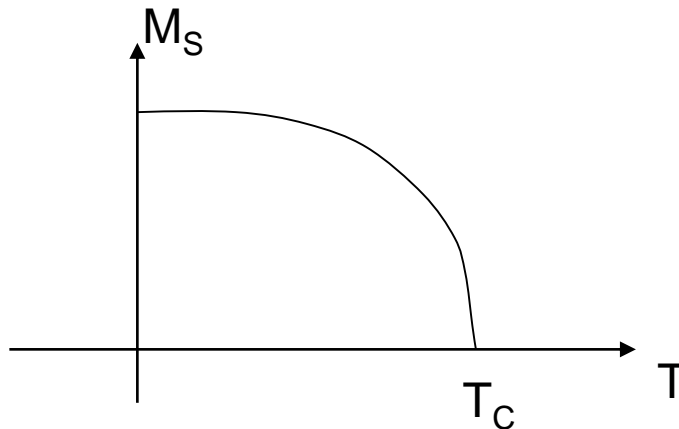


Fe, Co, Ni, alloys also with TM, C, and RE



Phase transition ferromagnet \rightarrow paramagnet

$\rightarrow M_s (T)$



Above a critical temperature called Curie temperature (T_C) all ferromagnets become regular paramagnets $\rightarrow M_S = 0$ at $\mathbf{H} = 0$

$$M_S \propto (T_C - T)^\beta \quad T < T_C$$

$\beta = 1/2$ mean field theory (identical average exchange field felt by all spins)

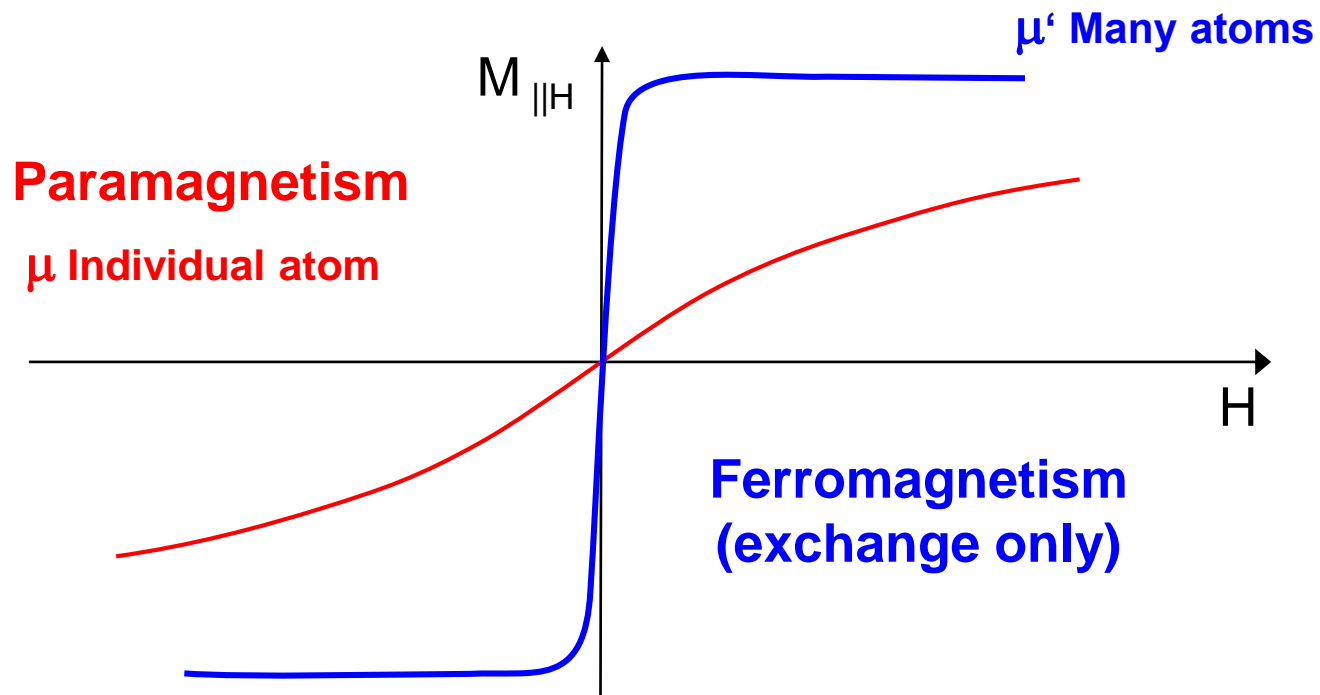
This temperature for anti-ferromagnets is called Néel temperature (T_N)



Origin of hysteresis

Ferromagnetic order not enough

Zeeman energy $E_m = -\mu_0 \mu \cdot \mathbf{H}$



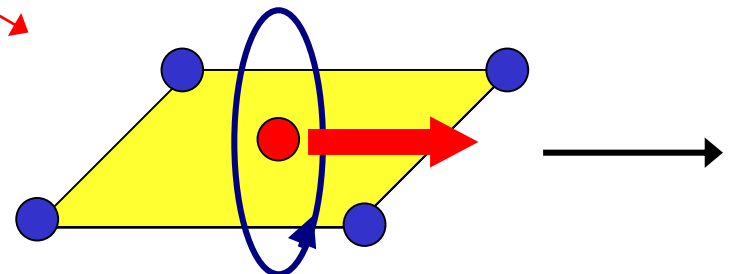
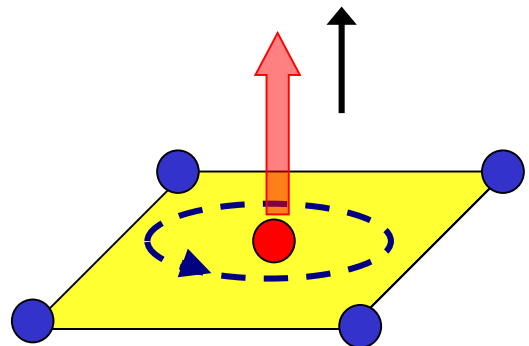
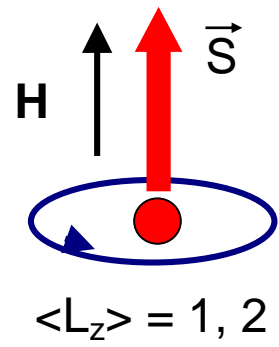
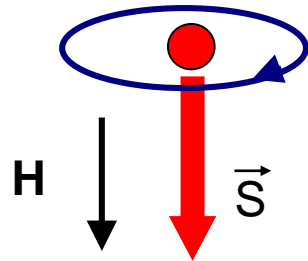


Magneto-crystalline anisotropy: spin-orbit coupling

Spin-orbit coupling tends to induce an orbital motion as sketched...but there is the crystal field potential.

d-orbital momentum in an atom

$$\langle L_z \rangle = -1, -2$$





- **Magnetocrystalline anisotropy**: dependence of internal energy on the direction of spontaneous magnetization respect to crystal axis. It is due to anisotropy of spin-orbit coupling energy and dipolar energy. Examples:

- Cubic $E_{anis} = K_1 (\alpha_x^2 \alpha_y^2 + \alpha_y^2 \alpha_z^2 + \alpha_z^2 \alpha_x^2) + K_2 \alpha_x^2 \alpha_y^2 \alpha_z^2 + \dots$

- Uniaxial $E_{anis} = K_1 \sin^2\theta + K_2 \sin^4\theta + \dots \approx -K_1(\mathbf{n} \cdot \mathbf{M})^2$

- **Surface and interface anisotropy**: due to broken translation symmetry at surfaces and interfaces. The surface energy density can be written:

- $E_{surf} = K_p \alpha_f^2 - K_s \alpha_n^2$; where α_n and α_f are the director cosines respect to the film normal and the in plane hard-axis.

- **Strain anisotropy**: strain distorts the shape of crystal (or surface) and, thus can give rise to an uniaxial term in the magnetic anisotropy.

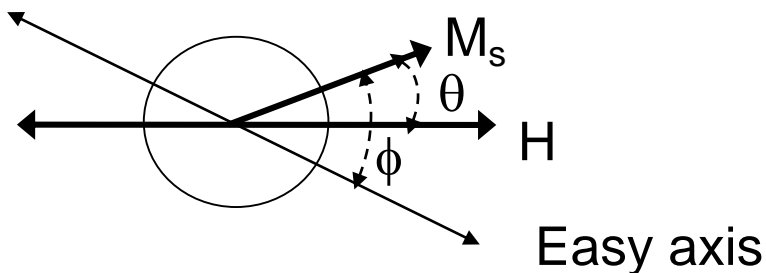
- $E_s = 3/2 \lambda \sigma \sin^2\theta$; where λ is the magnetostriction coefficient (positive or negative) along the direction of the applied stress σ and θ is the angle between the magnetization and the stress direction.

- **Growth induced anisotropy**: preferential magnetization directions can be induced by oblique deposition or by application of an external magnetic field during deposition.



Exchange+anisotropy → Hysteresis

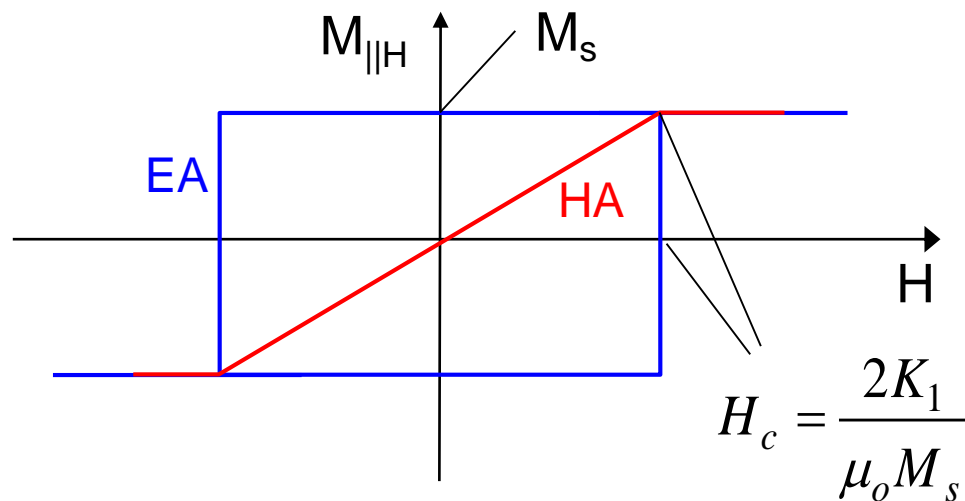
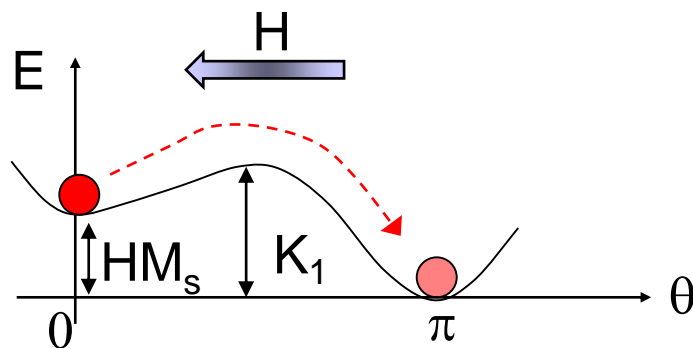
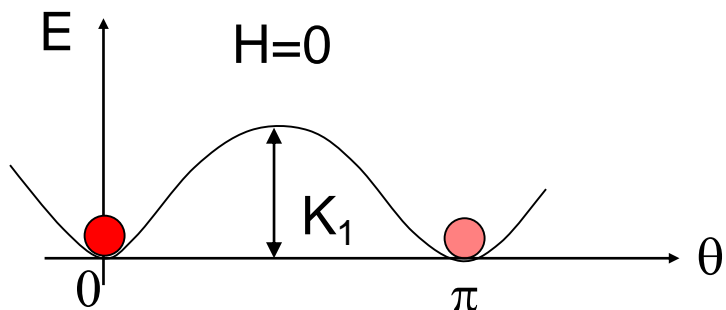
Bistable one-dimensional potential: uniaxial anisotropy



Stoner and Wohlfarth model

$$E_{tot} = E_{appl} + E_{anis}$$

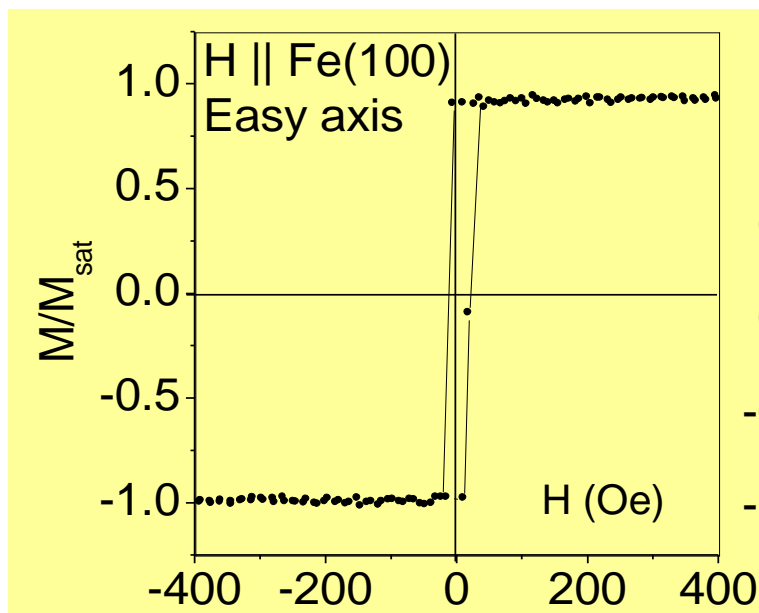
$$E_{tot} = K_1 \sin^2\phi - \mu_0 M_s H \cos\theta$$



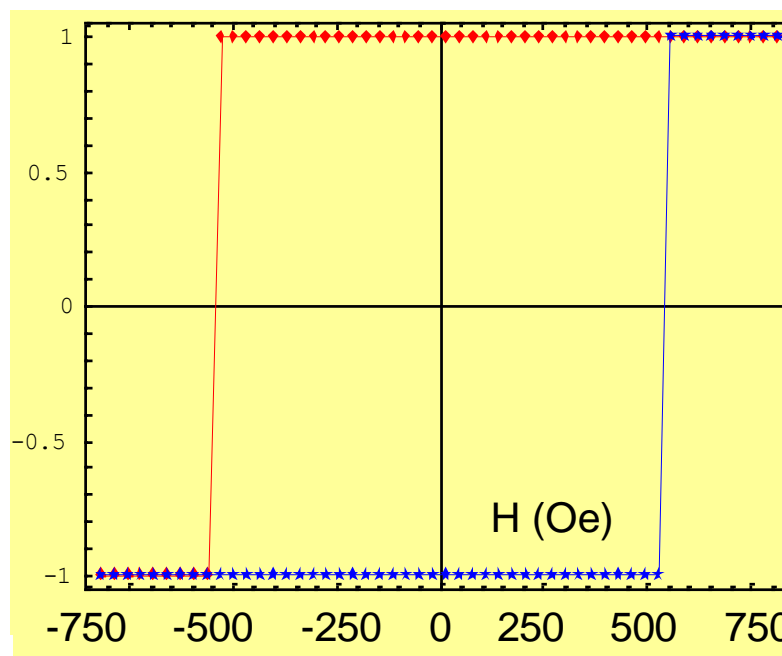


Exchange+anisotropy \rightarrow Hysteresis Real systems

Measured EA loop



Expected EA loop (anisotropy field 282 Oe:
 $K = 48000 \text{ J/m}^3$ Ms $1.7 \cdot 10^6 \text{ A/m} \rightarrow 28.2 \text{ mT}$)



Why this difference? Different reversal process: reversed domains nucleation



Magnetostatic energy.

Magnetostatic energy is potential energy of magnetic moments in the field \mathbf{H}_d they have created themselves.

The magnetostatic energy \mathcal{E}_m can be evaluated as:

$$\mathcal{E}_m = \frac{1}{2} \mu_0 \iiint_{\text{all space}} H_d^2(r) d^3 r = -\frac{1}{2} \mu_0 \iiint_{\text{sample}} \mathbf{M}(r) \cdot \mathbf{H}_d(r) d^3 r \geq 0$$

If for simplicity we assume that \mathbf{M} is uniform inside the body the integral becomes a surface integral where \mathbf{H}_d can be thought as produced by surface magnetic charges

$\sigma_s = \mathbf{M} \cdot \mathbf{n}$ and the energy \mathcal{E}_m depends solely on the shape of the body.

The uniformity condition can be realized only for isotropic ellipsoids and for such special cases $\mathbf{H}_d = -\mathbf{N} \mathbf{M}$, where \mathbf{N} is a tensor called demagnetizing tensor.

Referring to the ellipsoid semi-axes the tensor becomes diagonal and the diagonal elements N_x, N_y, N_z are called demagnetizing factors and $N_x + N_y + N_z = 1$

Magnetostatic self interaction for an ellipsoid (referring to the ellipsoid semi-axes)

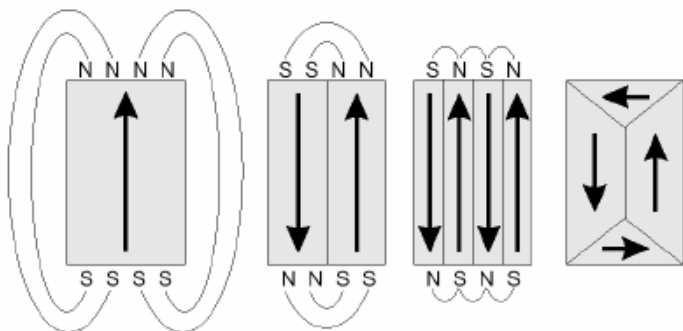
$$\mathcal{E}_m = 1/2 \mu_0 (N_x M_x^2 + N_y M_y^2 + N_z M_z^2).$$



Magnetostatic energy: why magnetic domains form.

The magnetization of a sample may be split in many *domains*.

Each of these domains is magnetized to the saturation value M_s but the direction of the magnetization vector may vary from one domain to the other at $\mathbf{H} = 0$.



Energy densities

In vacuum

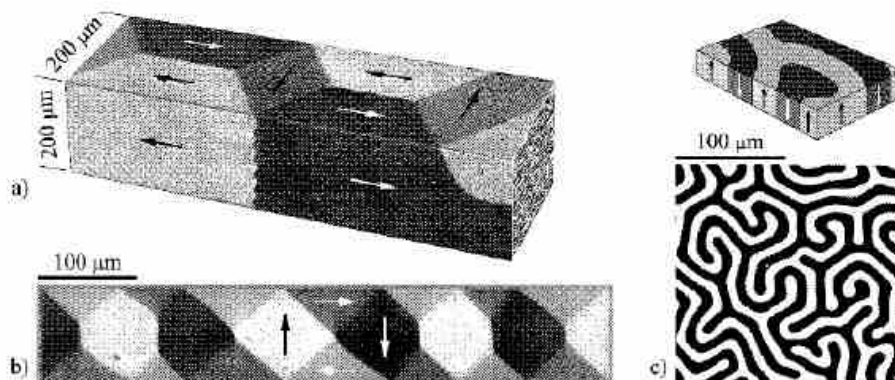
$$u = B^2/2\mu_0$$

Inside a material

$$u = 1/2 \mu_0 M_s^2$$

Total energy

$$U = \iiint_{\text{All space}} u dt$$



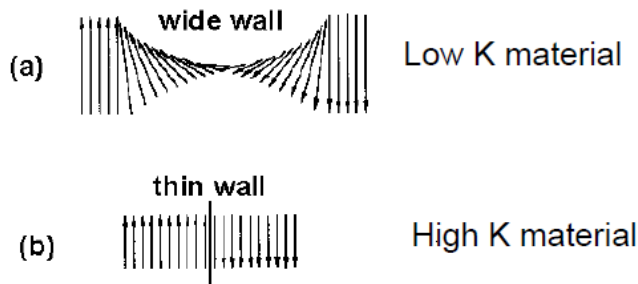
There is a cost for magnetic domains formation

Wall width

Usual expressions normalized by the spin quantum number:

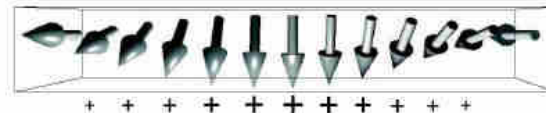
Domain wall width $w \propto \sqrt{J/K}$

Domain wall energy $E \propto \sqrt{J \cdot K}$



Domain wall orientation

A **Bloch wall** in a thin films generates stray fields in the outside region, which is unfavourable.



Néel walls become more favourable when the film thickness t becomes smaller than the wall width w : $t < w$

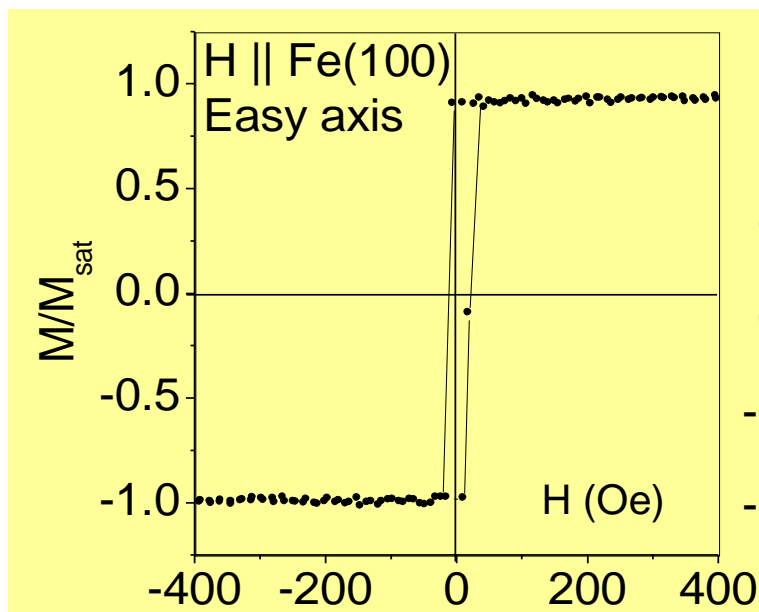


In both cases a 180° domain wall is shown with a wall width stretching over the box size.

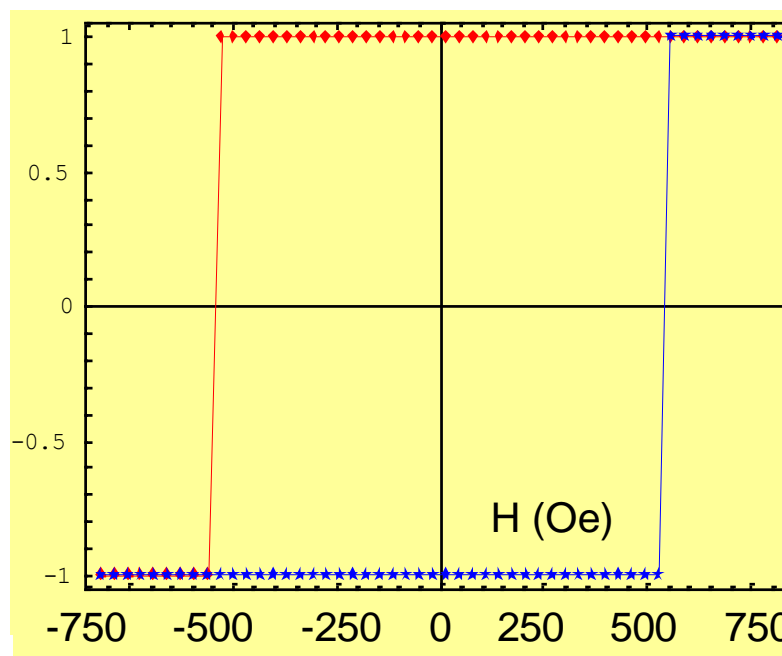


Exchange+anisotropy \rightarrow Hysteresis Real systems

Measured EA loop



Expected EA loop (anisotropy field 282 Oe: $K = 48000 \text{ J/m}^3$ Ms $1.7 \cdot 10^6 \text{ A/m} \rightarrow 28.2 \text{ mT}$)



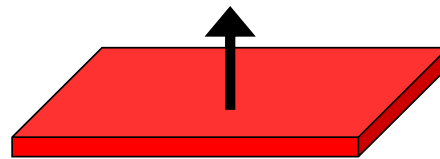
Why this difference? Different reversal process: reversed domains nucleation



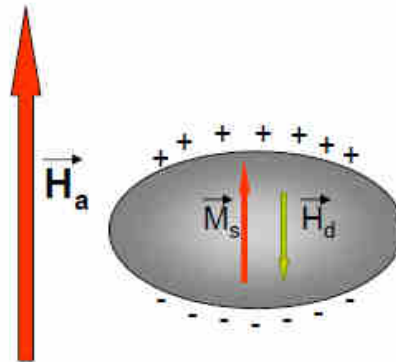
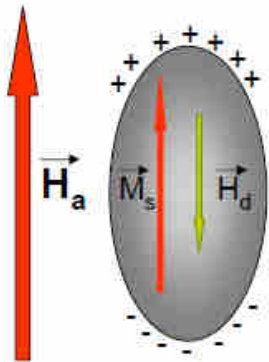
Magnetostatic energy: Shape anisotropy



favoured



unfavoured



Equivalent to an uniaxial anisotropy

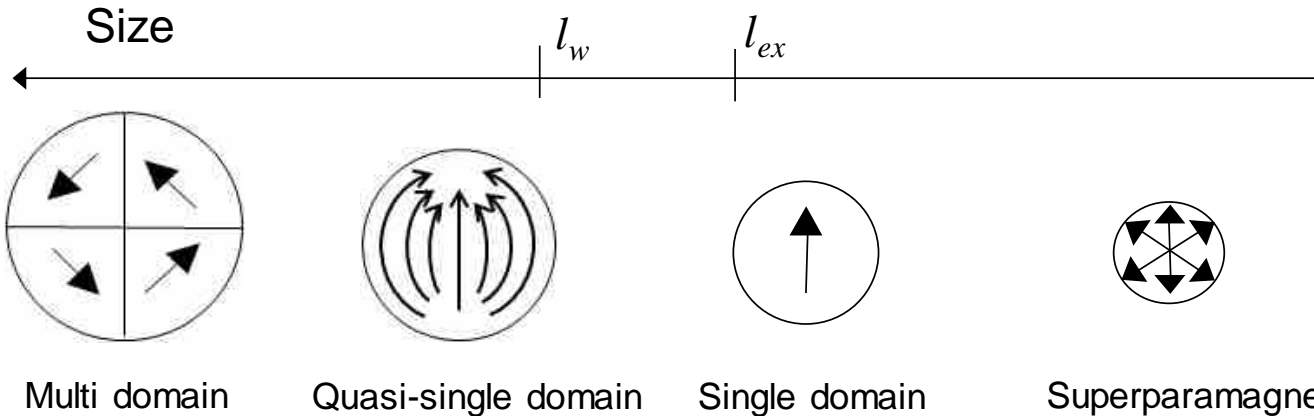
$$K_s = 1/2 \mu_0 M_s^2 (N_{\perp} - N_{\parallel})$$

$$H_d = N_{\parallel} M_s \leftarrow \vec{H}_d = -N_d \vec{M} \rightarrow H_d = N_{\perp} M_s$$

Osborne PRB 67, 351 (1945)



Size and shape effects



Characteristic lengths

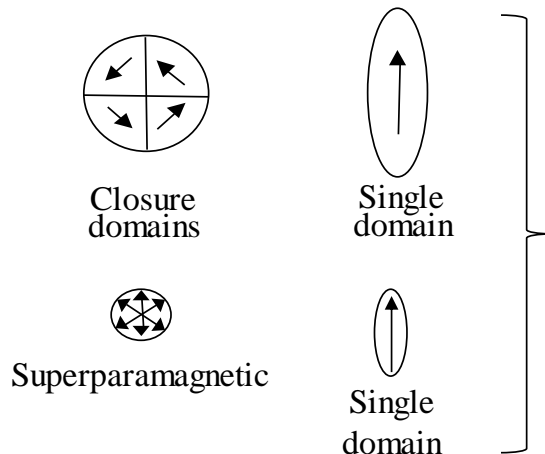
$$l_w = \sqrt{A/K_1}$$

$$l_{ex} = \sqrt{2A/\mu_0 M_s^2}$$

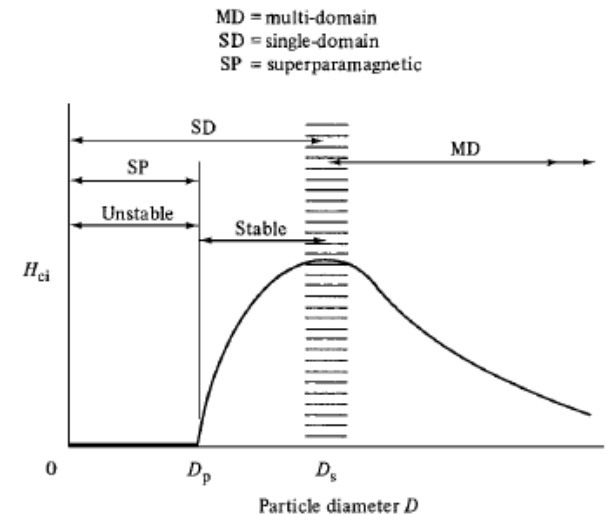
Exchange stiffness
 $A \propto J$

Shape

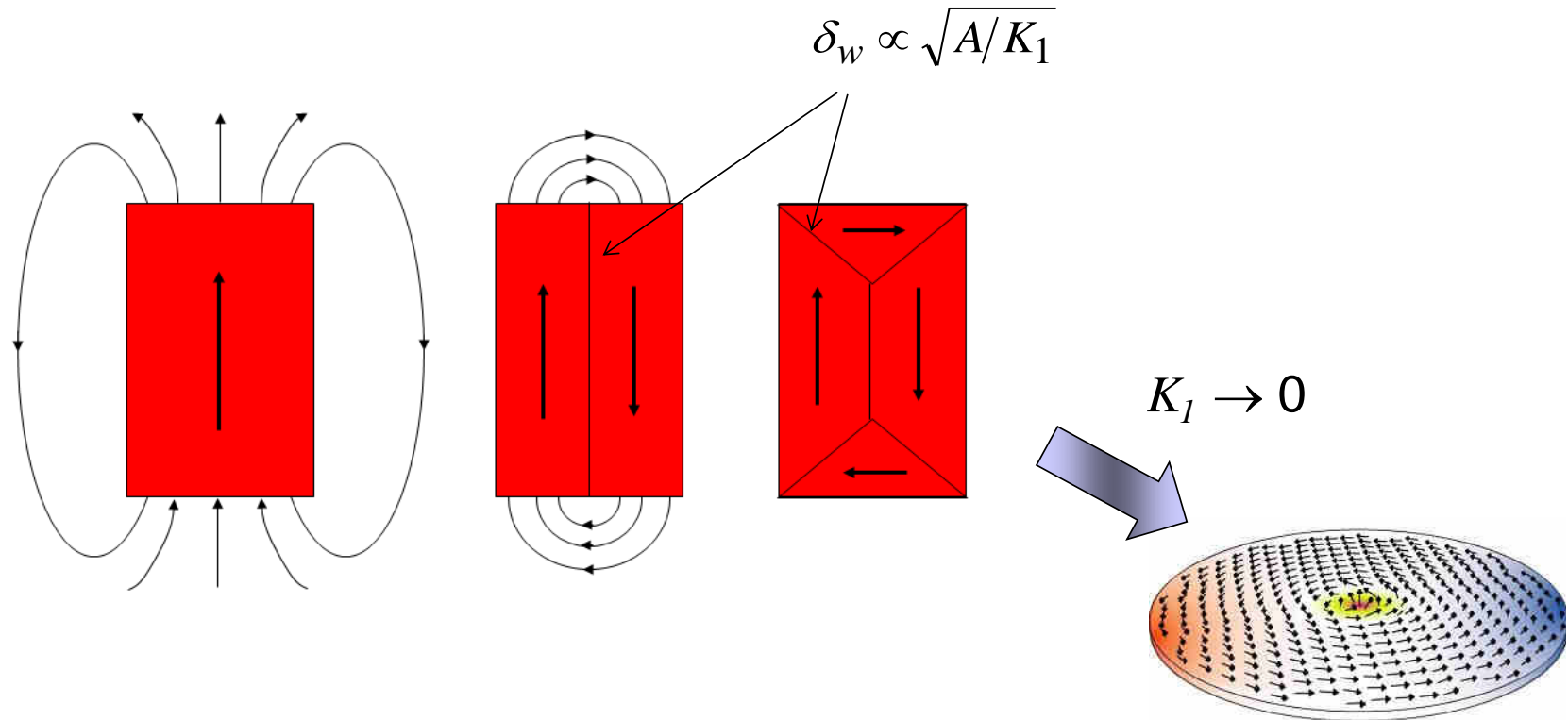
Aspect ratio effects



Very helpful!
It extends the size (volume range for single domain behaviour!
Utilized in applications.



Exotic magnetization states in nanostructures



Magnetic vortex



Thermal stability of the remanent state: superparamagnetism

Superparamagnetic limit

Below a certain size (blocking volume V_B), islands behave in a superparamagnetic fashion. M is homogeneous but fluctuates with the period:

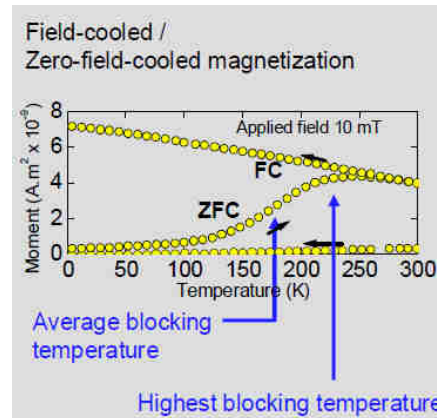
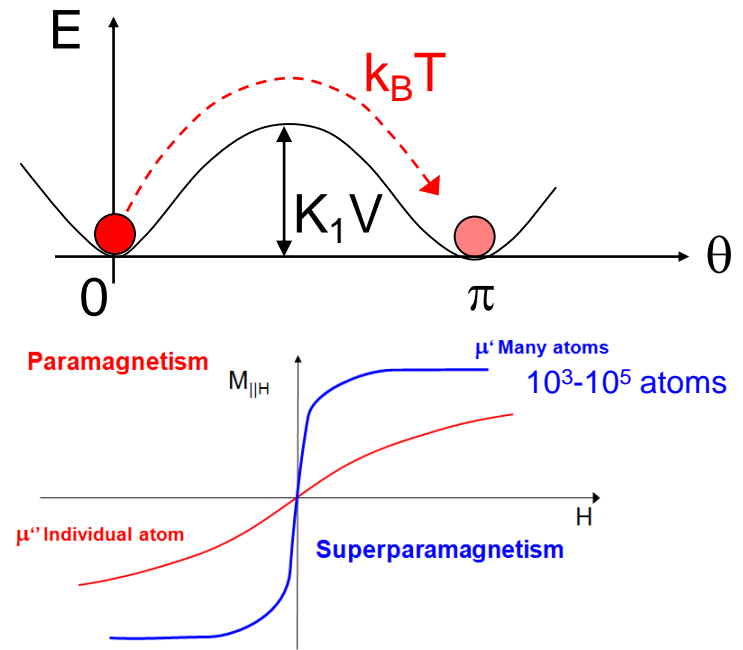
$$\tau = \tau_0 e^{E_K/k_B T}, E_K = K_u V_B$$

E_K is the stored crystal anisotropy in a particle.
For $T < T_B$, the spin blocks freeze out, for $T > T_B$, the remanent magnetization M_R vanishes.
For magnetic recording, a particle energy of $E_K = K_u V_B > 55 k_B T$ is required for a 10 year stability.

$$\tau_0 \approx 10^{-10} \text{ s}$$

$$\tau = 1 \text{ s for } E_K \approx 23 k_B T$$

Blocking T , $T_B \approx E_K/23k_B$, is the T at which for a given particle (fixed E_K) $\tau = 1 \text{ s}$, which is the typical measurement time.



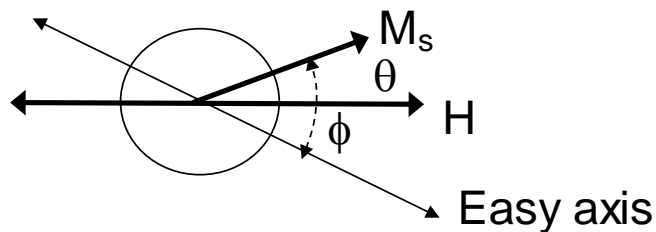
M.F. Hansen, S. Mørup,
J. Magn. Magn. Mater. 203, 214-216 (1999)

Serious issue for magnetic recording



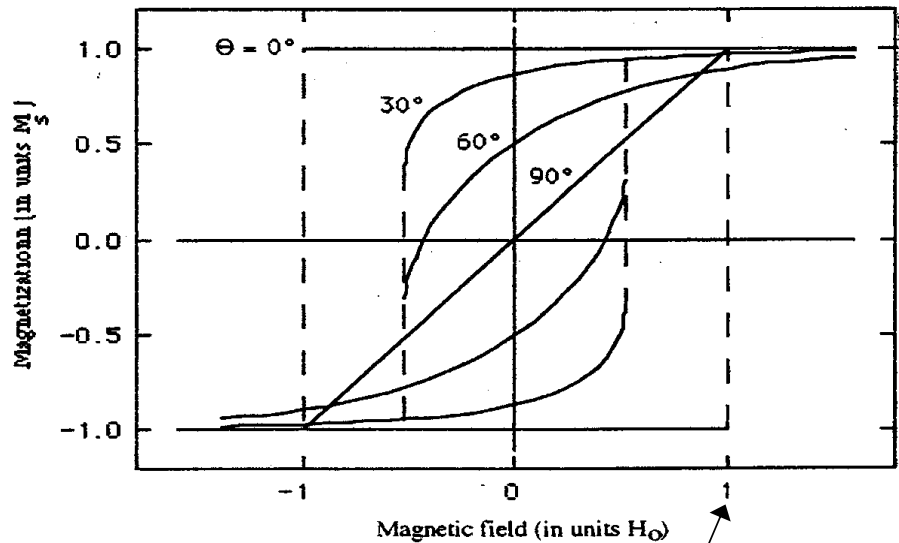
Coherent rotation

Stoner and Wohlfarth model: coherent rotation of an uniaxial particle uniformly magnetized.



$$E = K_1 \sin^2\phi - \mu_0 M_s H \cos\theta$$

Free energy for unit volume

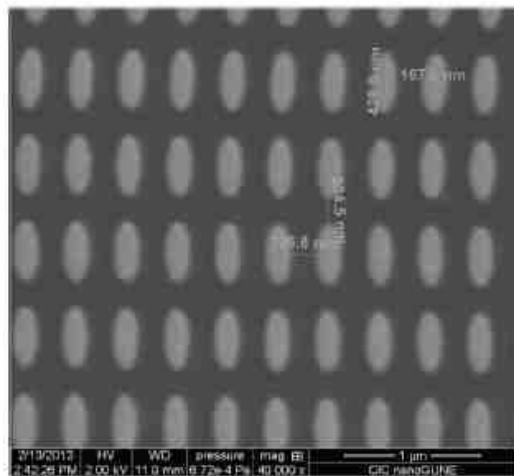


$$H_0 = \frac{2K_1}{\mu_0 M_s}$$



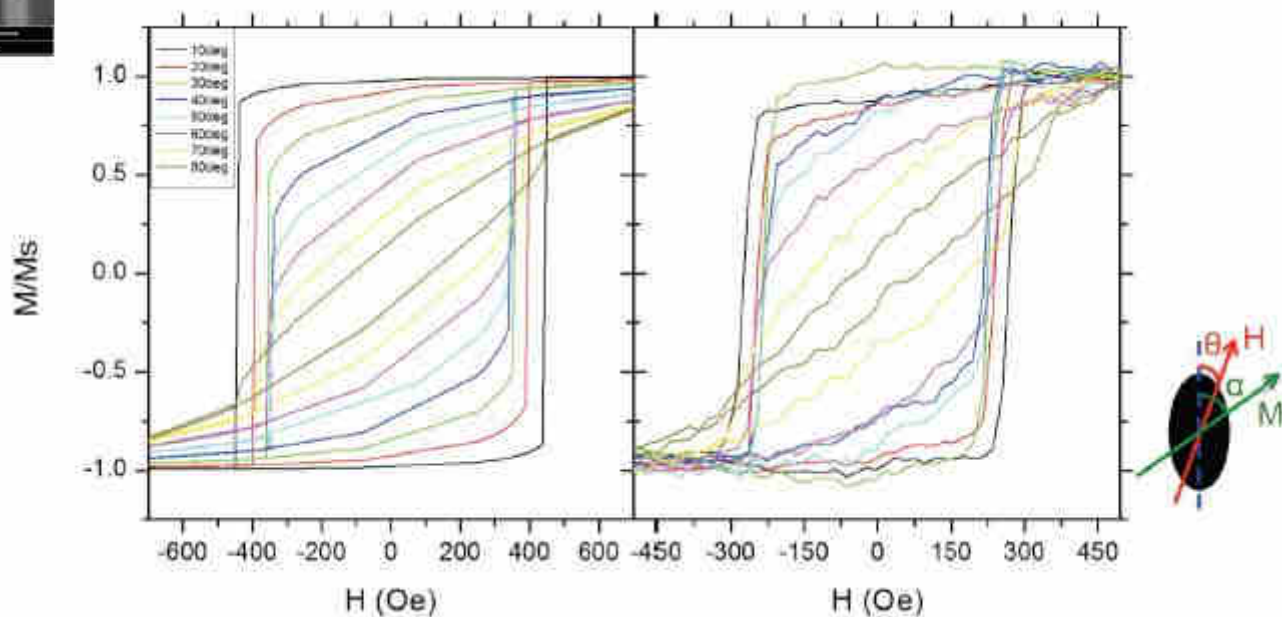
Coherent rotation in nanomagnets

FeNi elliptical nanostructures



S&W model

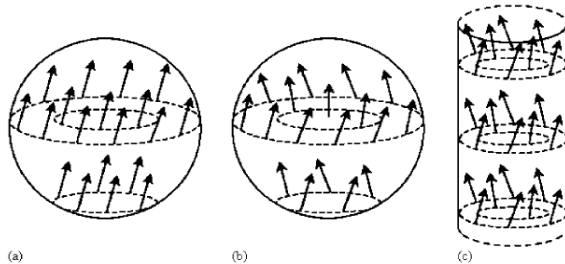
Experiment (MOKE)





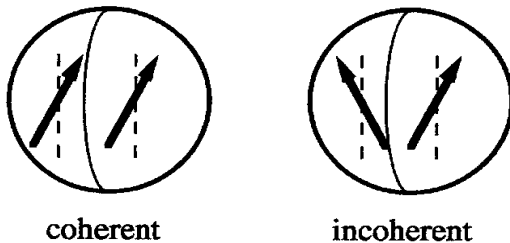
Incoherent vs. coherent reversal

For single domain particles the reversal process can be still incoherent, in a way different from domain wall displacement: **curling mode (Brown)**.



Coherent and incoherent reversal

Here: nucleation in a sphere

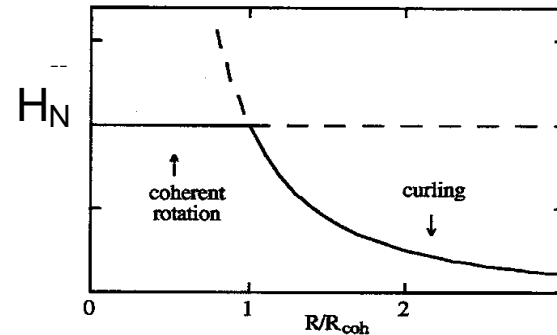


Coherent rotation below $R_{coh} = 5.099 \sqrt{A/\mu_0 M_s^2}$:

$$H_N = \frac{2K_1}{\mu_0 M_s}$$

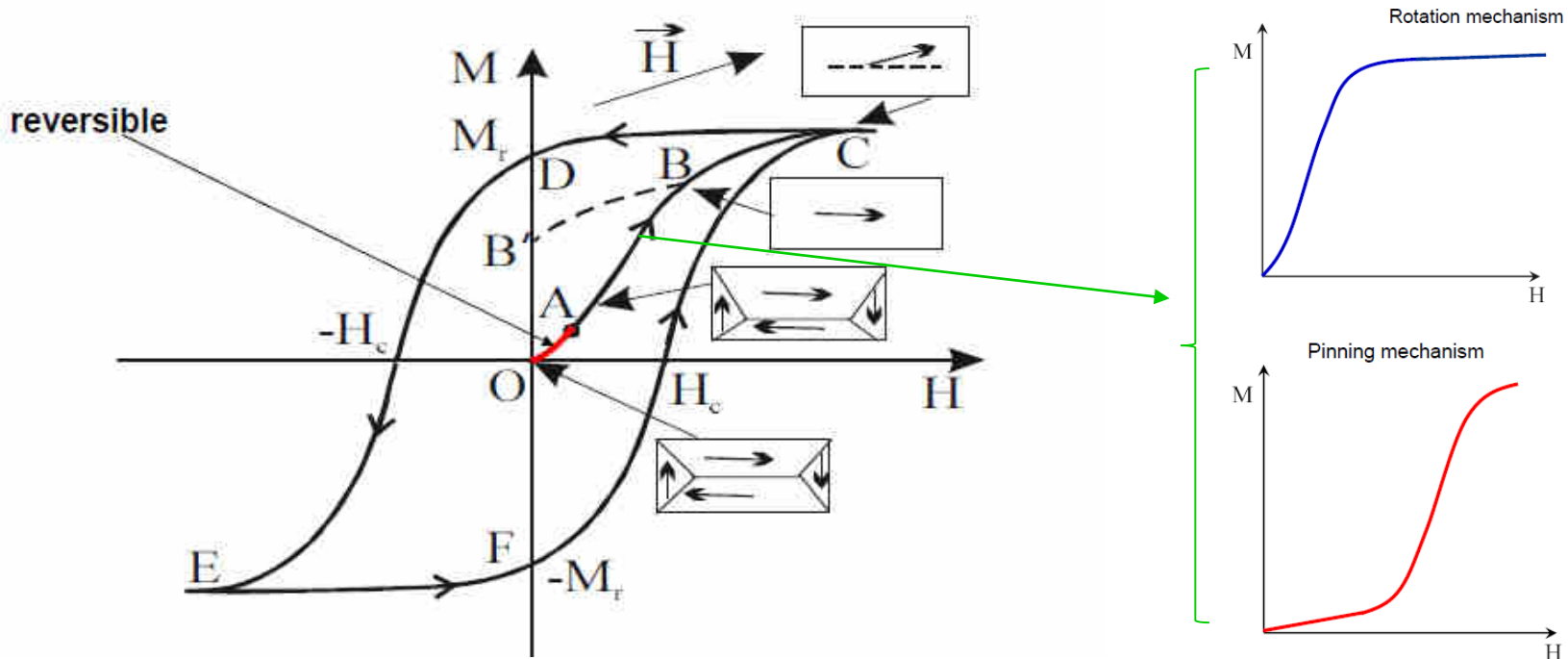
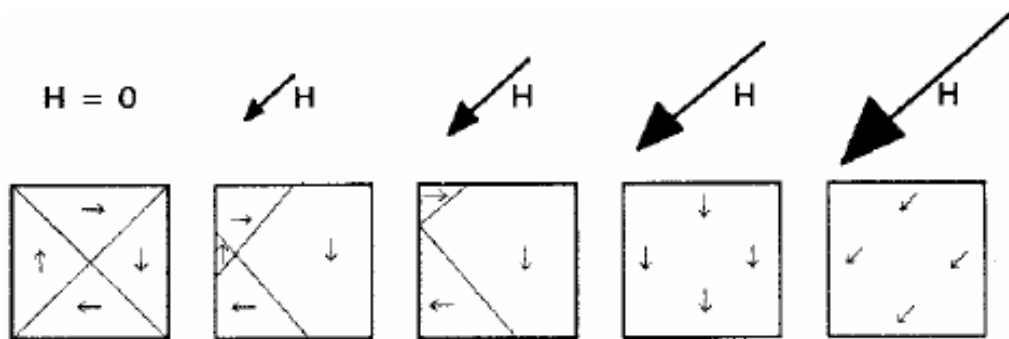
Incoherent nucleation (curling) above R_{coh}

$$H_N = \frac{2K_1}{\mu_0 M_s} - \frac{1}{3} M_s + \frac{8.666 A}{\mu_0 M_s R^2}$$





Magnetization reversal and domains

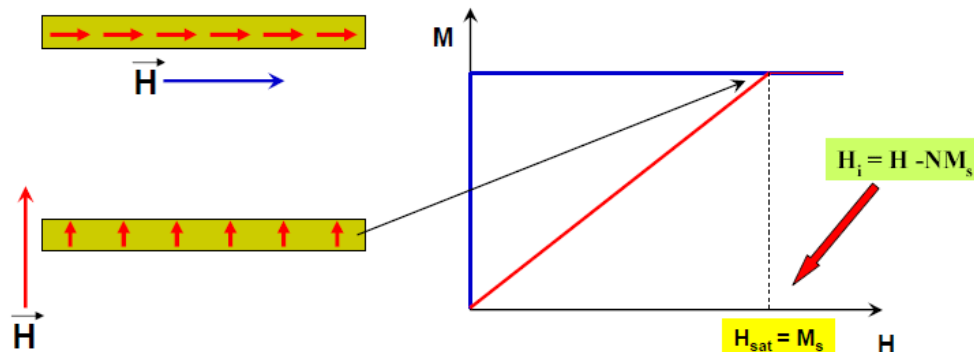




What can be derived from hysteresis loops

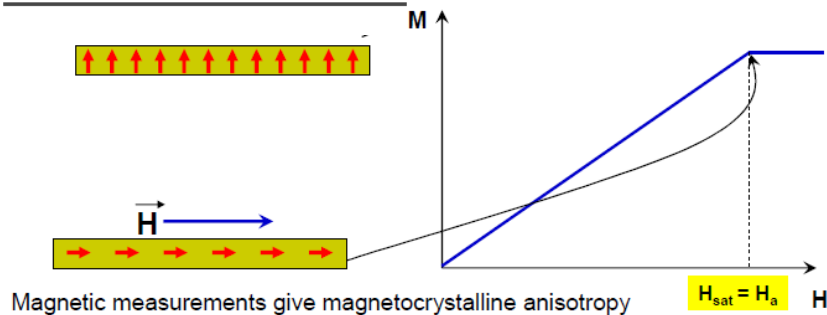
magnetic measurements on *plate shape samples*

NO MAGNETOCRYSTALLINE ANISOTROPY



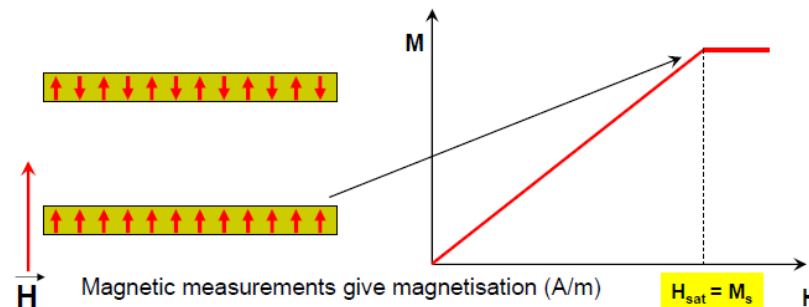
Magnetic measurements give magnetisation (A/m)

PERPENDICULAR ANISOTROPY



Magnetic measurements give magnetocrystalline anisotropy

$H_{sat} = H_a$



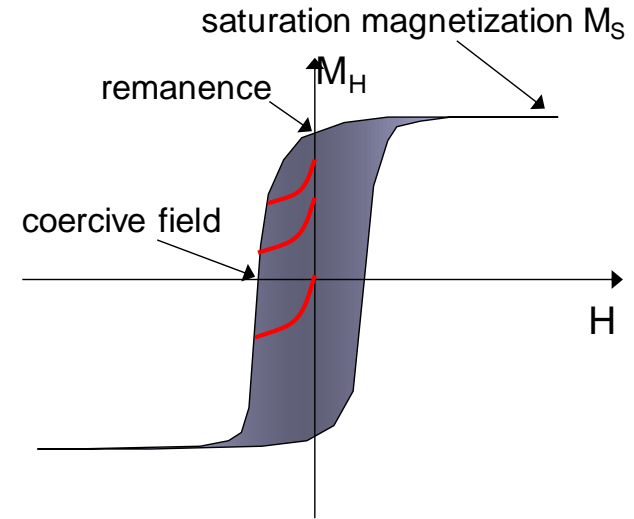
Magnetic measurements give magnetisation (A/m)

$H_{sat} = M_s$

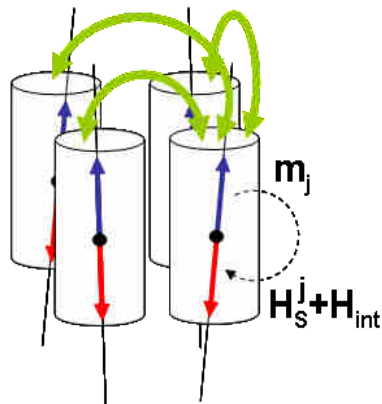


What can be derived from hysteresis loops

There is a lot of valuable information beyond that contained the limiting hysteresis curve (major hysteresis loop).



Grain assembly:
with competing interactions



Based on this idea, a number of quantitative tools has been developed to investigate the “switching field distribution” (SFD) and interaction field distribution in granular materials (magnetic recording).

Examples are: the $\Delta H(M, \Delta M)$ -Method, Henkel-plots, FORC, SORC.....

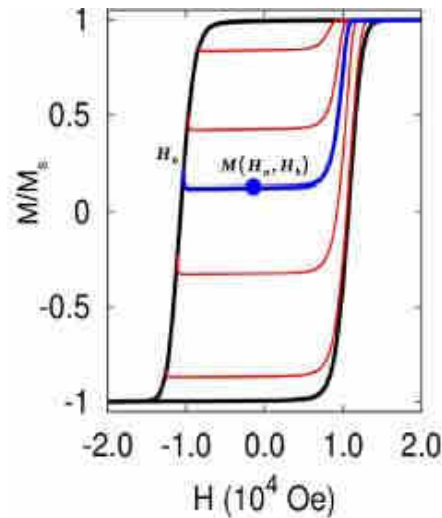
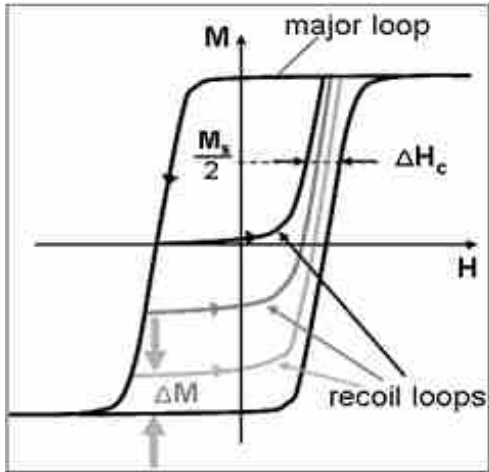
Tagawa, I. & Nakamura, Y. Relationships between high density recording performance and particle coercivity distribution. IEEE Trans. Magn. 27, 4975–4977 (1991).

Liu, Y., Dahmen, K. & Berger, A. Determination of intrinsic switching field distributions in perpendicular recording media: Numerical study of the $\Delta H(M, \Delta M)$ method. Phys. Rev. B 77, 054422 (2008).



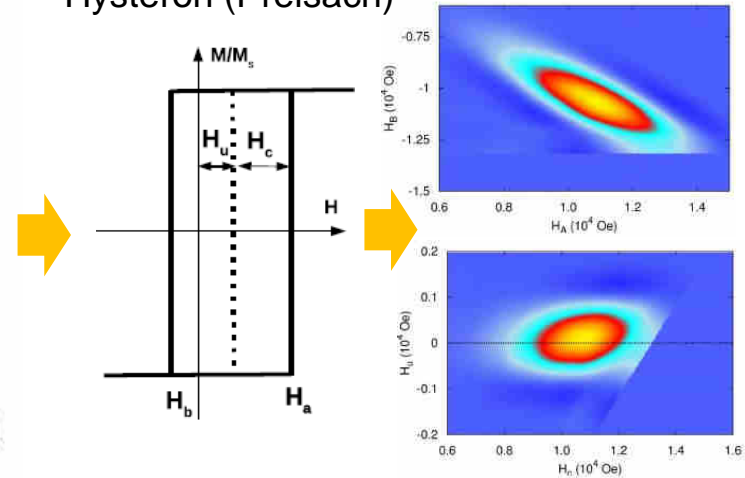
What can be derived from hysteresis loops

$\Delta H(M, \Delta M)$ and ΔH_c methods



FORC

Hysteron (Preisach)



Measurement protocol used to generate the FORC data:

- The starting point is the saturation of the sample by applying a large positive applied field. The field is then decreased towards the reversal field, H_b , when the field direction is reversed and increased from H_b back to positive saturation. This process generates a FORC attached to the major hysteresis loop at the reversal point H_b . The magnetisation point at an applied field $H_a > H_b$ along this FORC, denoted as $M(H_a, H_b)$, is internal to the major hysteresis loop. As illustrated, at any value of H_a in the hysteresis region, there is an entire family of such internal magnetisation points $M(H_a, H_b)$ distinguished by the reversal field H_b of their corresponding FORCs.
- The FORC data are then analysed by computing the numerical second-order derivative of the functional dependence $M(H_a, H_b)$ with respect to the applied field H_a and H_b .

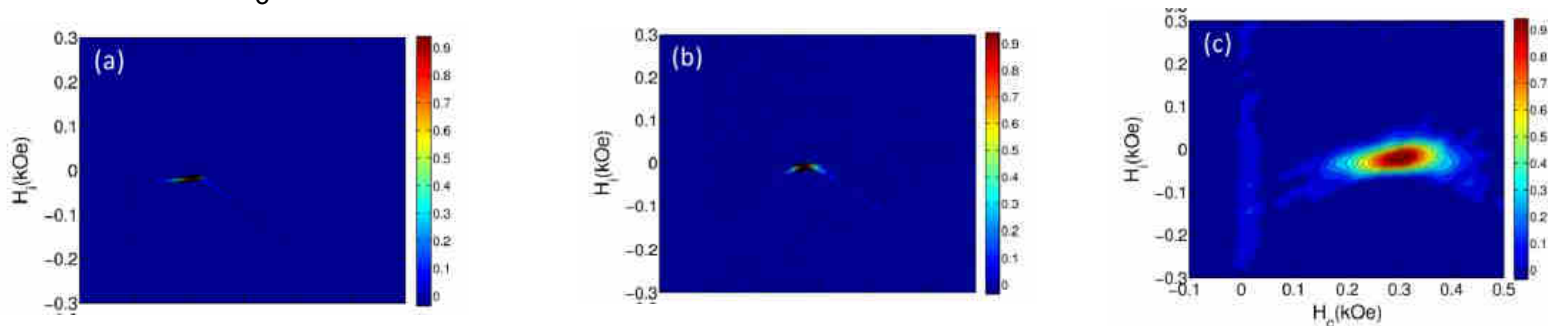
$$\rho_{ab}(H_a, H_b) = -\frac{1}{2M_s} \frac{\partial^2 M(H_a, H_b)}{\partial H_a \partial H_b}$$

A FORCs diagram is a contour plot of equation



What can be derived from hysteresis loops: FORC

It is conventional (and useful) to transform ρ_{ab} introducing new variables $H_c = (H_b - H_a)/2$ and $H_u = (H_b + H_a)/2$, which are the coercive and bias (also identified with H_i , interaction) fields, allowing one to capture the reversible magnetization component, which appears to be centered in $H_c = 0$.



H_c and H_u are essentially the coercive and bias (interaction) fields of the hysteron.

The SFD can be obtained by a straightforward integration over the variable H_u :

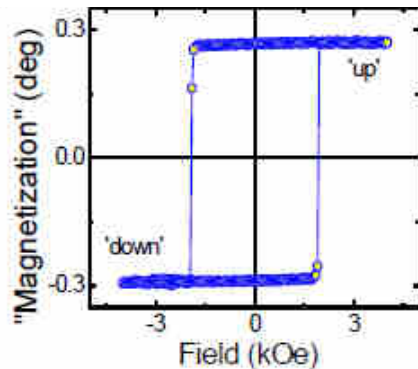
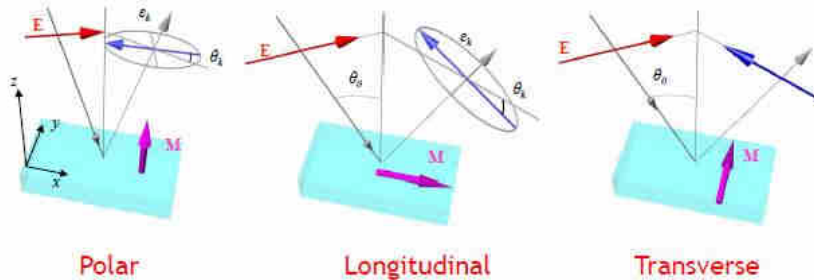
$$\rho_{\text{SFD}}(H_c) = \int_{-\infty}^{\infty} \rho(H_c, H_u) dH_u$$

- Mayergoyz, I. D. Hysteresis models from the mathematical and control theory points of view. J. Appl. Phys. 57, 3803 (1985).
- Winklhofer, M. & Zimanyi, G. T. Extracting the intrinsic switching field distribution in perpendicular media: A comparative analysis. J. Appl. Phys. 99, 08E710 (2006).
- Stancu, A., Pike, C., Stoleriu, L., Postolache, P. & Cimpoesu, D. Micromagnetic and Preisach analysis of the First Order Reversal Curves (FORC) diagram. J. Appl. Phys. 93, 6620 (2003).

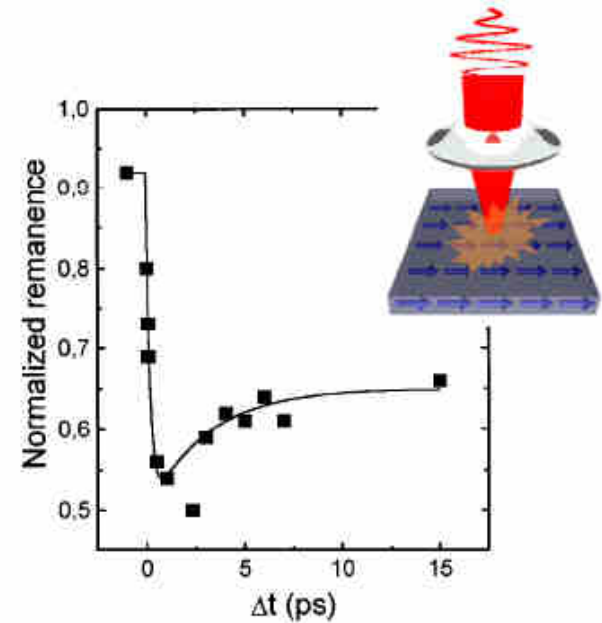


MOKE magnetometry

What could be measured?



hysteresis



Beaurepaire et al. PRL 76, 4250 (1996).

dynamics

surface/interface sensitivity



Important caveat

● not everything you measure is magnetization

VOLUME 85, NUMBER 4

PHYSICAL REVIEW LETTERS

24 JULY 2000

Ultrafast Magneto-Optics in Nickel: Magnetism or Optics?

B. Koopmans,* M. van Kampen, J. T. Kohlhepp, and W. J. M. de Jonge

*Eindhoven University of Technology, Department of Applied Physics, COBRA Research Institute,
P.O. Box 513, 5600 MB, Eindhoven, The Netherlands*

(Received 22 February 2000)

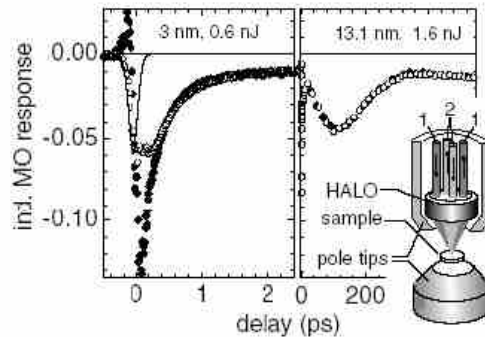


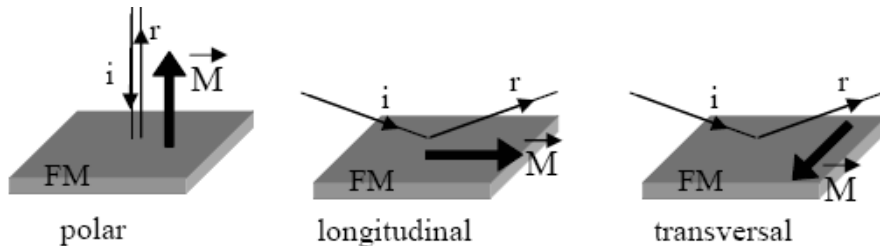
FIG. 1. Comparison of the induced ellipticity ($\Delta\psi''/\psi_0''$, open circles) and rotation ($\Delta\psi'/\psi_0'$, filled diamonds) as a function of pump-probe delay time, for a (111) oriented film at the thicknesses and pulse energies indicated. The thick line represents the pump-probe cross correlation trace. The inset depicts the experimental configuration with pump ("1") and probe ("2") beams.

$$\frac{\Delta\theta(t)}{\theta_0} = \frac{\Delta\varepsilon(t)}{\varepsilon_0} = \frac{\Delta M(t)}{M_0}$$

system out of equilibrium



MOKE magnetometry: characteristics



The magneto-optic Kerr effect (MOKE) is widely used in studying technologically relevant magnetic materials.

It relies on small, magnetization induced changes in the optical properties which modify the polarization or the intensity of the reflected light.

Macroscopically, magneto-optic effects arise from the antisymmetric, off-diagonal elements in the dielectric tensor.

$$\hat{\epsilon} = \begin{bmatrix} \epsilon_0 & 0 & 0 \\ 0 & \epsilon_0 & 0 \\ 0 & 0 & \epsilon_0 \end{bmatrix} \longrightarrow \hat{\epsilon} = \begin{bmatrix} \epsilon_0 & i\epsilon_z & -i\epsilon_y \\ -i\epsilon_z & \epsilon_0 & i\epsilon_x \\ i\epsilon_y & -i\epsilon_x & \epsilon_0 \end{bmatrix}$$

$$\epsilon_x = \epsilon_0 Q m_x; \quad \epsilon_y = \epsilon_0 Q m_y; \quad \epsilon_z = \epsilon_0 Q m_z;$$



- Non-destructive;
- High sensitivity;
- Finite penetration depth (~ 10 nm);
- Fast (time resolved measurements);
- Laterally resolved (microscopy);
- Can be easily used in vacuum and cryogenic systems;

J. Kerr, Philosophical Magazine 3 321 (1877)

Z. Q. Qui and S. D. Bader, Rev. Sci. Instrum. 71, 1243 (2000)

Fresnell reflection coefficients

$$\text{Sample} \begin{pmatrix} r_{pp} & r_{ps} \\ r_{sp} & r_{ss} \end{pmatrix} \quad \begin{aligned} r_{pp} &= r_{pp}^0 + r_{pp}^M \propto m_y \\ r_{ps} &\propto -m_x - m_z \\ r_{sp} &\propto m_x - m_z \end{aligned}$$

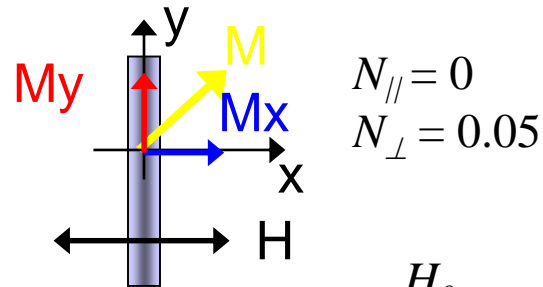
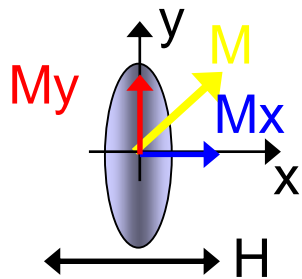
$$r_{pp} = \frac{E_{rTM}}{E_{iTM}} \quad r_{ps} = \frac{E_{rTM}}{E_{iTE}} \quad r_{sp} = \frac{E_{rTE}}{E_{iTM}} \quad r_{ss} = \frac{E_{rTE}}{E_{iTE}}$$

P. Vavassori, APL 77 1605 (2000)



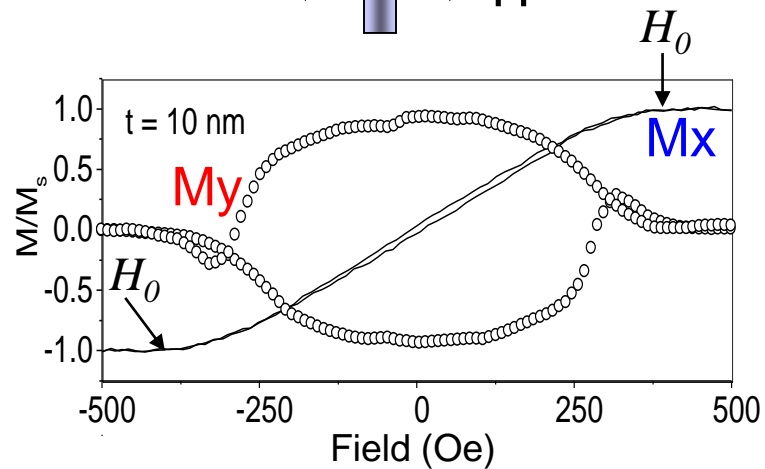
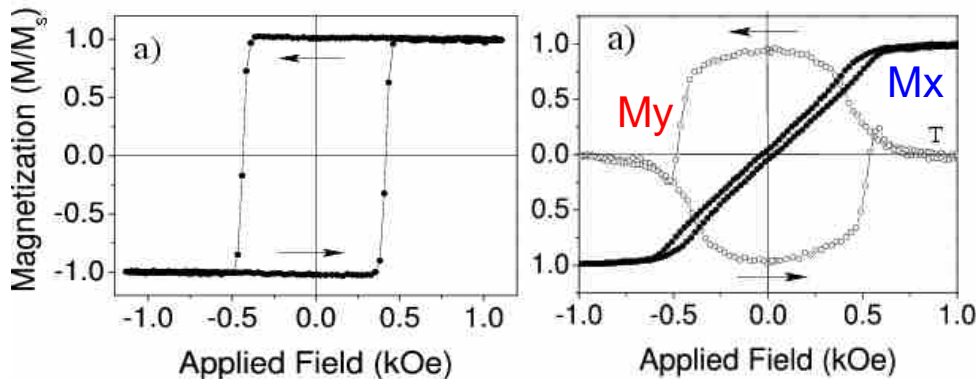
Vector MOKE magnetometry

Reversal in elongated ellipses and wires (FeNi) for H applied along the short axis (hard direction). The process is now almost coherent.



$$N_{||} = 0$$

$$N_{\perp} = 0.05$$



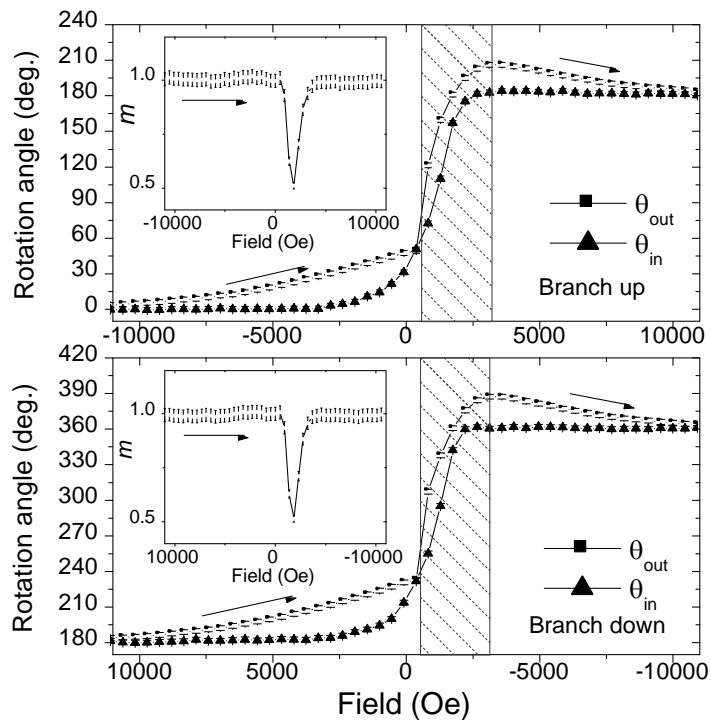
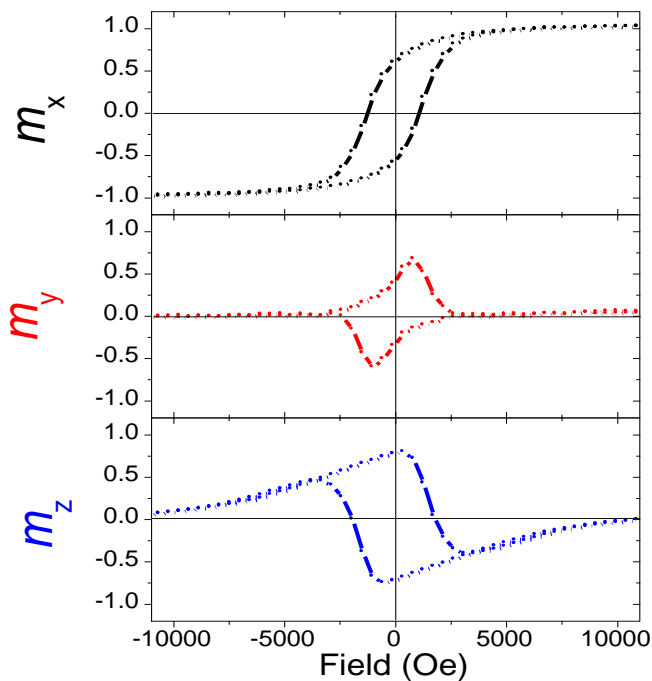
$$K_s = 1/2 \mu_0 M_s^2 (N_{\perp} - N_{||}) = 0.025 \mu_0 M_s^2$$

$$H_0 = \frac{2K_1}{\mu_0 M_s} = 0.05 * M_s \rightarrow M_s = 650 \text{ kA/m}$$



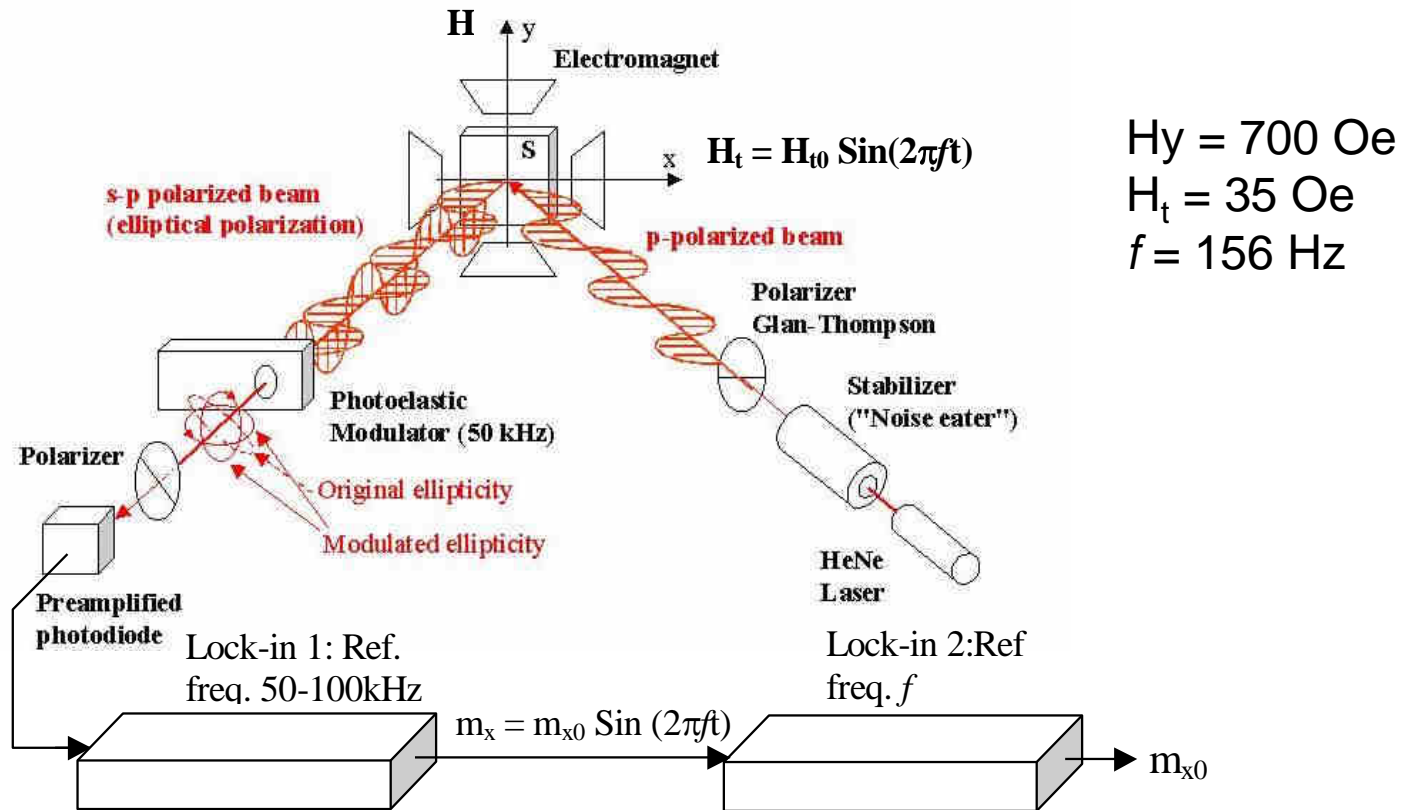
Vector MOKE 3D magnetometry

180-nm-thick CoNiO



P. Vavassori, Appl. Phys. Lett. **77**, 1605 (2000)

MOKE transverse susceptibility setup: anisotropy



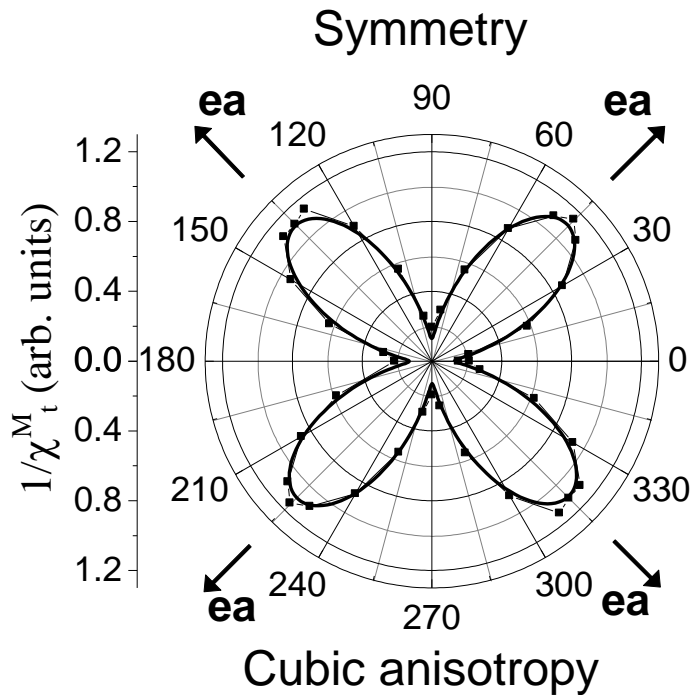
The quantity measured with the Lock-in 2 is proportional to the transverse susceptibility $\chi_t = \Delta\theta_0 / H_{t0}$.

It can be shown that: $1/\chi_t = (E_o''(\theta_{eq}) / \langle M \rangle_{eq})$ where $E_o(\theta_{eq})$ is the total free energy and $\langle M \rangle_{eq}$ is the average magnetization, which makes an angle θ_{eq} with the EA.

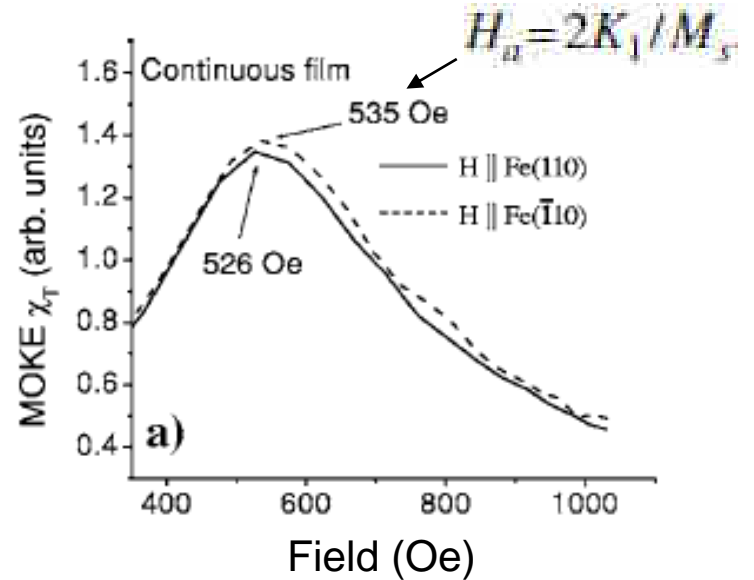


Continuous film: fit to a $\sin^2(2\theta)$ function

Epitaxial, 10 nm-thick Fe film on MgO(001) single crystal, with its (100) axis parallel to the (110) direction of the substrate.



Anisotropy field \rightarrow Energy

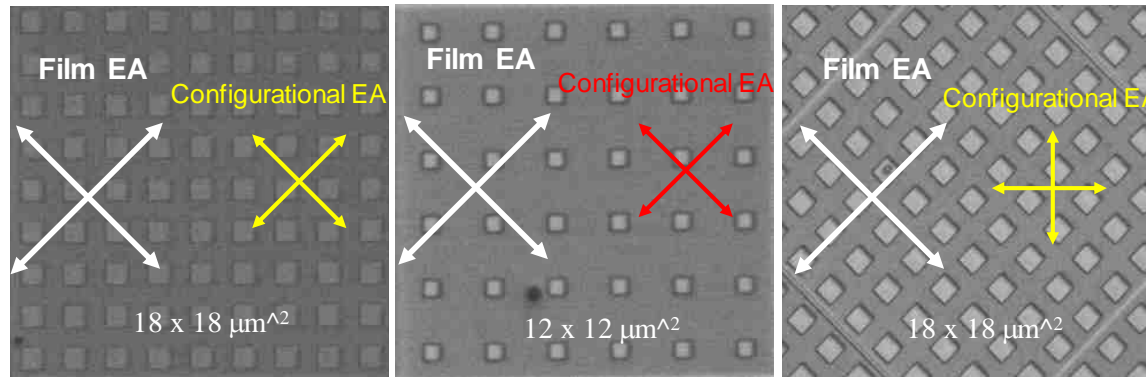


$$K_1 = 47.5 \cdot 10^3 \text{ J/m}^3$$



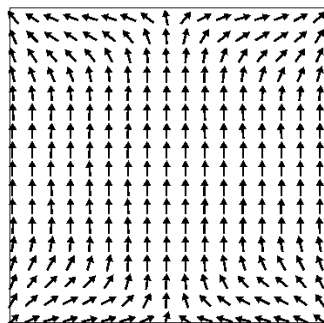
Configurational anisotropy symmetry

Epitaxial, 10 nm-thick Fe film on MgO(001) single crystal, with its (100) axis parallel to the (110) direction of the substrate. To avoid oxidation, the whole film has been capped with a 10 nm MgO film. A Focused Ion Beam has been subsequently used to selectively remove portion of the bilayer to produce the different arrays (the area of each array is $50 \times 50 \mu\text{m}^2$).

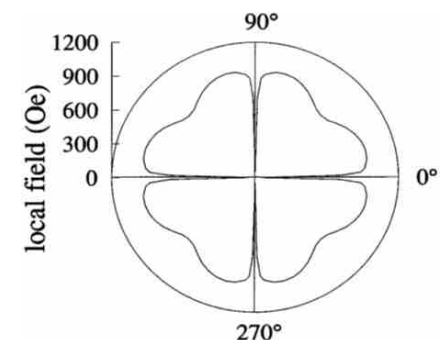
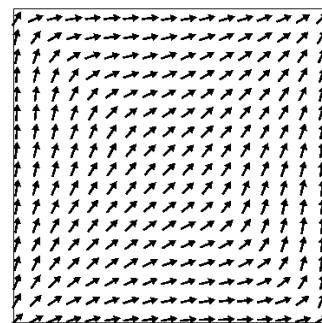


For a square element it has a **fourfold** symmetry, at first order, and **eightfold** symmetry at higher order. This higher order term becomes more important as the size of the element is reduced.

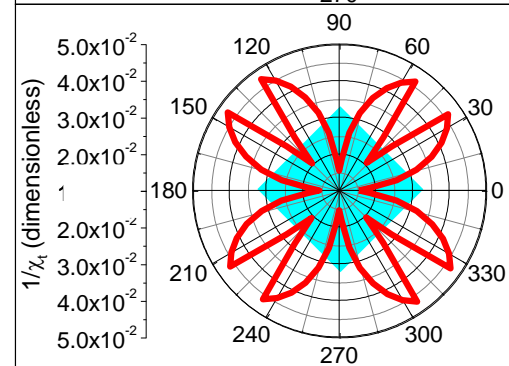
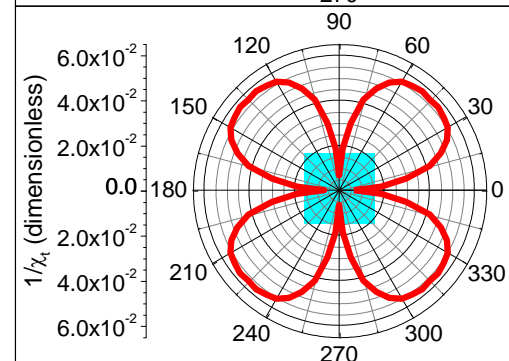
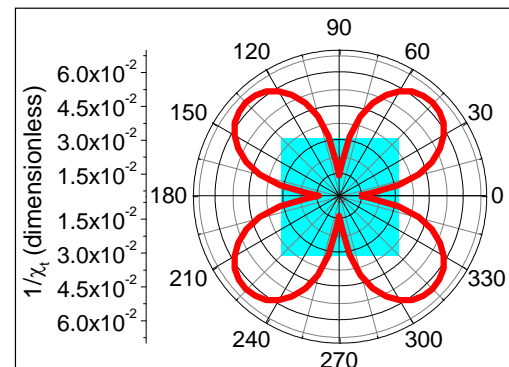
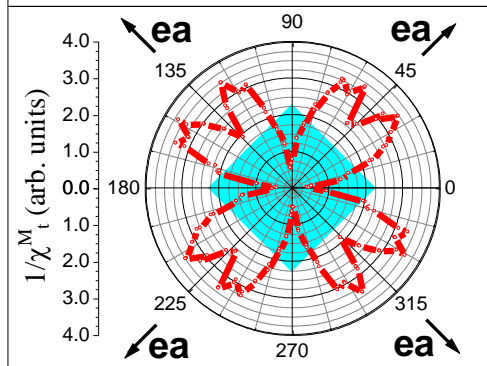
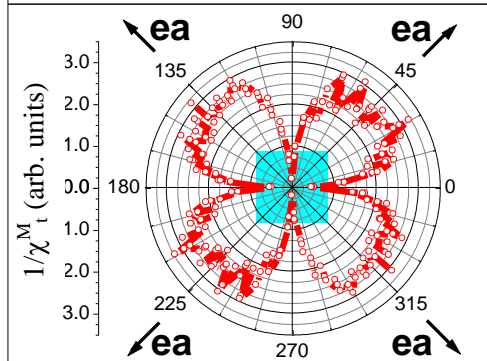
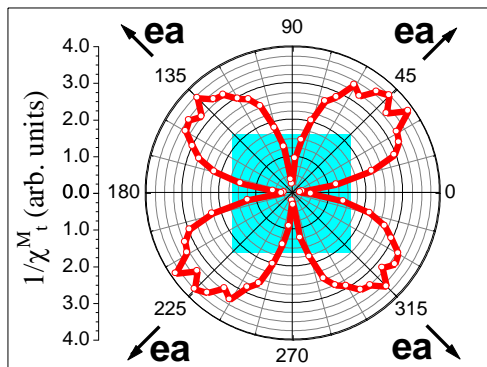
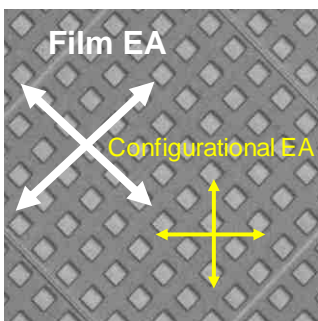
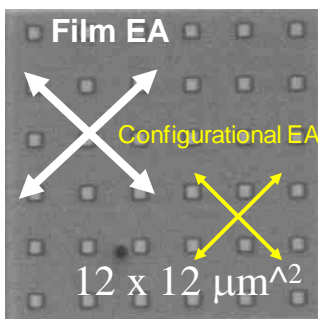
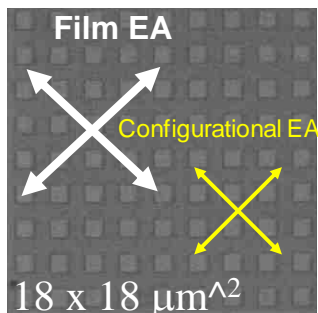
Flower state: higher energy



Leaf state: lower energy



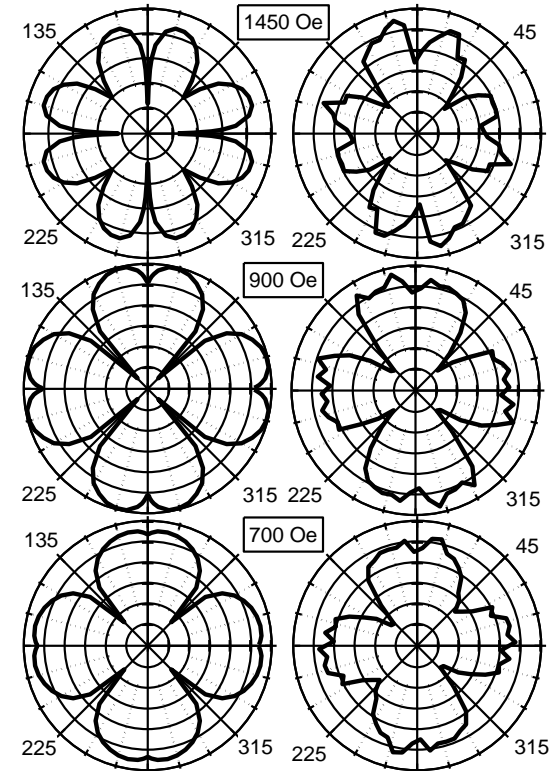
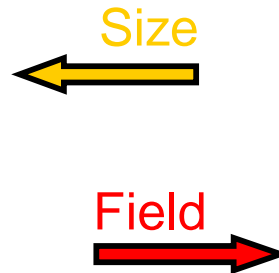
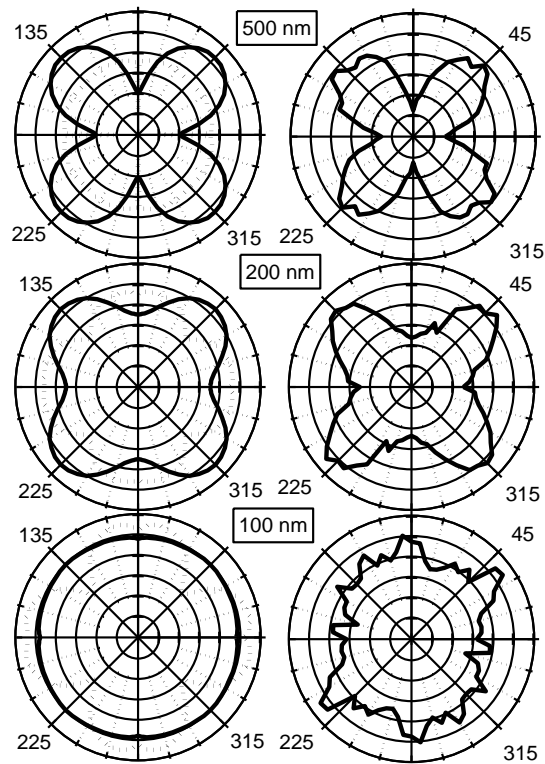
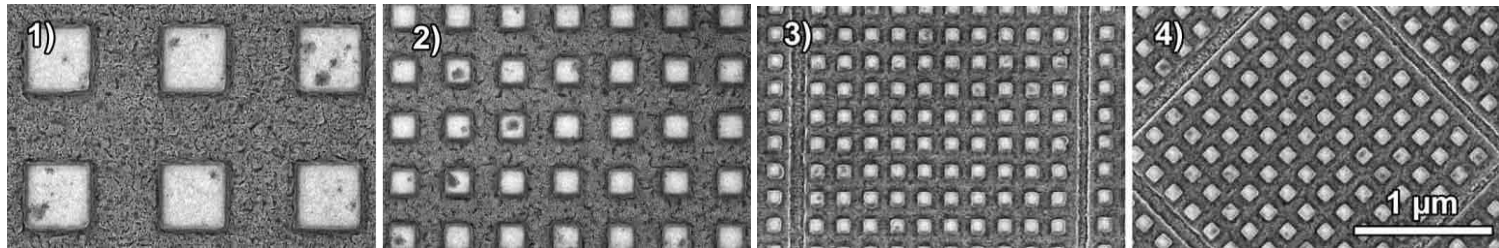
R. P. Cowburn et al. Phys. Rev. Lett. 81, 5414 (1998)



P. Vavassori et al., PRB 72, 054405 (2005)



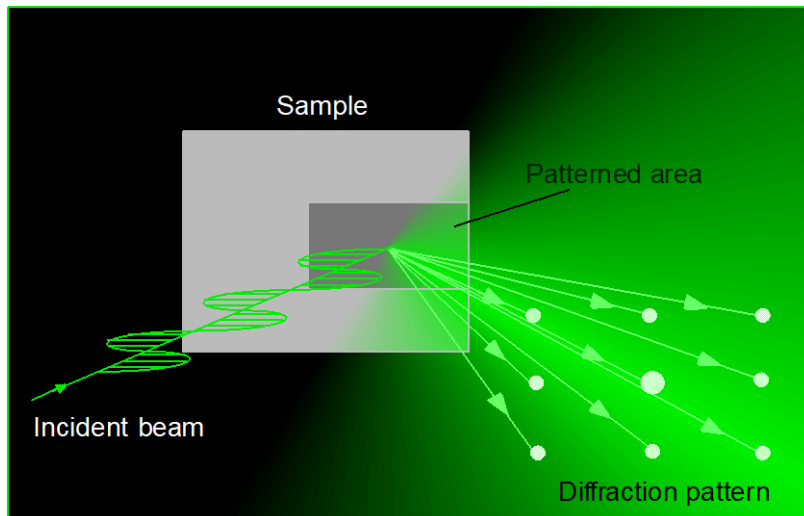
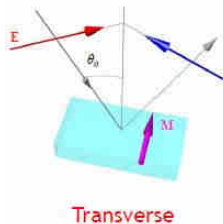
Size and bias field dependence



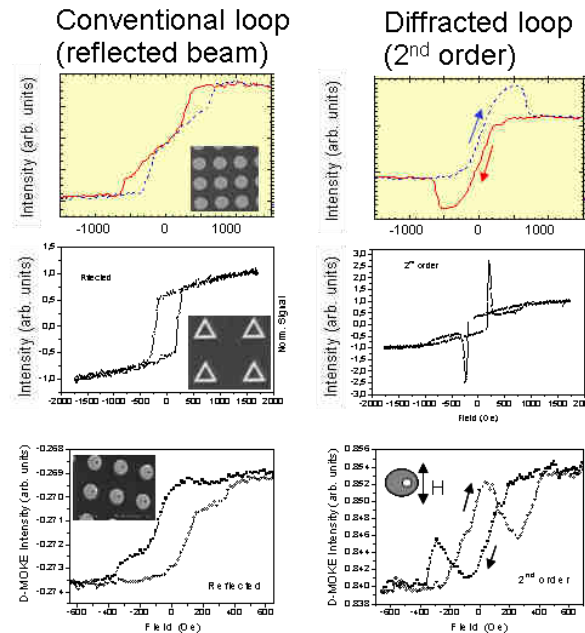
A. di Bona, S. F. Contri, G. C. Gazzadi, S. Valeri, and P. Vavassori, *J. Magn. Magn. Mater.* **316/2**, 106 (2007)



Diffraction-MOKE



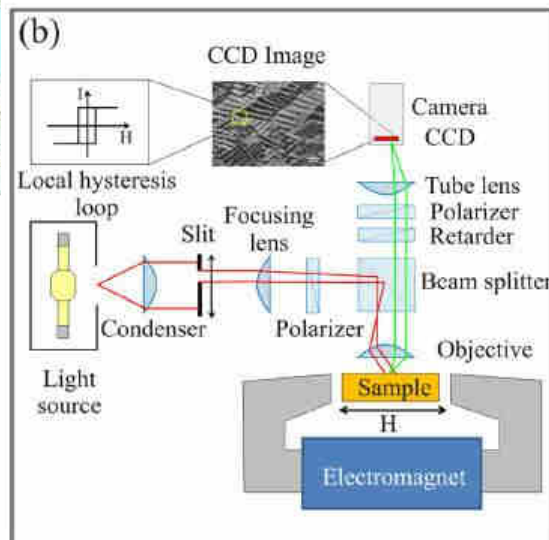
Peculiar structures due to
- Collective properties
- Interference effects



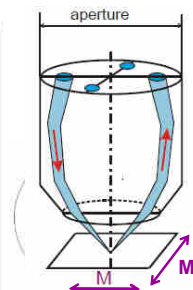
P. Vavassori, et al., Phys. Rev. B **59** 6337 (1999)
 M. Grimsditch, P. Vavassori, et al., Phys. Rev. B **65**, 172419 (2002)
 P. Vavassori, et al., Phys. Rev. B **67**, 134429 (2003)
 P. Vavassori, et al., Phys. Rev. B **69**, 214404 (2004)
 P. Vavassori, et al., J Appl. Phys. **99**, 053902 (2006)
 P. Vavassori, et al., J. Appl. Phys. **101**, 023902 (2007)
 P. Vavassori, et al., Phys. Rev. B **78**, 174403 (2008)
 T. Verduci et al., Appl. Phys. Lett. **99**, 092501 (2011)



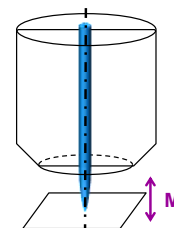
Ultrasensitive magnetometry with MOKE microscopy



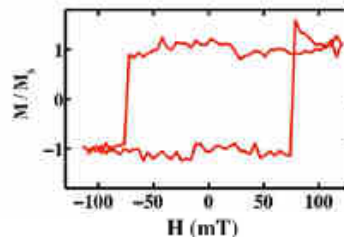
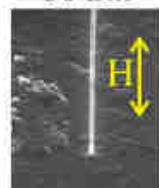
Longitudinal and transverse



Polar



30 nm



single sweep measurement sensitivity of approximately equal to sensitivity of 10^{-12} to 10^{-13} Am² for the latest generation of SQUID magnetometer

APPLIED PHYSICS LETTERS 100, 142401 (2012)



Required sensitivity for nanoscale magnetometry

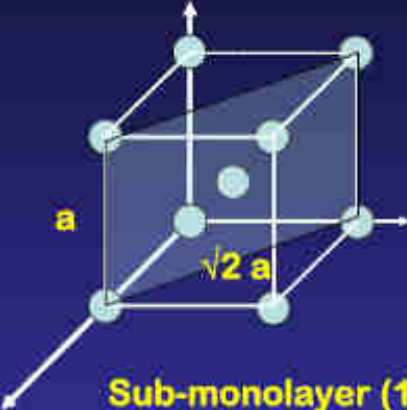
Spontaneous magnetization M_s of bulk elements

	bcc-Fe 286 K	hcp-Co 287 K	fcc-Ni 287 K
[kA / m]	1717	1447	493
[T]	2.16	1.82	0.62
[μ_B]	2.18	1.74	0.58



Required sensitivity for nanoscale magnetometry

Sub-monolayer films (ultra-thin films)



Example:
Fe / W(110), bcc (110),
 $a = 3.16 \text{ \AA}$

$n_{W(110)} = 1.42 \times 10^{15} \text{ cm}^{-2}$

Sub-monolayer (1% ML) sensitivity requires: $10^{13} \mu_B$
 10^{-10} J / T
 10^{-6} A cm^2

accurate magnetization data can only be derived for known amounts of deposited materials (e.g. thickness calibration)

$$\mu \sim 0.1 \mu_{\text{emu}}$$

Similar cases occur, for example, studying nanoparticles, dilute magnetic semiconductors (DMS), undoped oxides and superconductors, doped topological insulators, claimed to exhibit room temperature ferromagnetism (RT-FM) in thin-film or nanoparticle form.

However, an increasing number of reports suggest or even demonstrate that the observed ferromagnetism may originate from extrinsic sources, such as magnetic contamination or measurement artefacts.

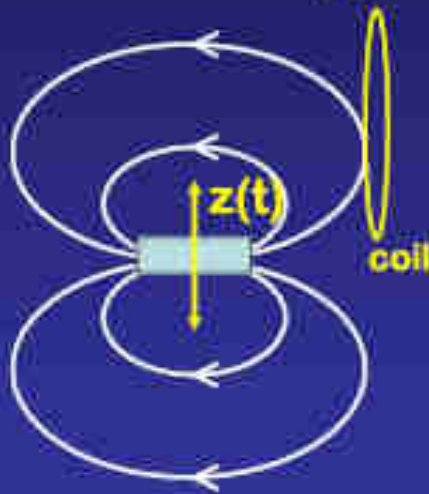


Vibrating sample magnetometer (VSM)

S. Foner, Rev. Sci. Instr. 30(1959)548; JAP 79(1996)4740.

a moving magnetized sample induces a voltage V in a pick-up coil

change of flux Φ is induced by the stray field B of the sample, which is approximated by a dipolar field



$$\Phi(t) = \iint_{\text{coil}} B_x(x_{\text{coil}}, y, z(t)) dy dz$$

$$V \sim \frac{d\Phi}{dt} \quad (\sim m_{\text{total}, x}) \quad \text{Faraday law}$$

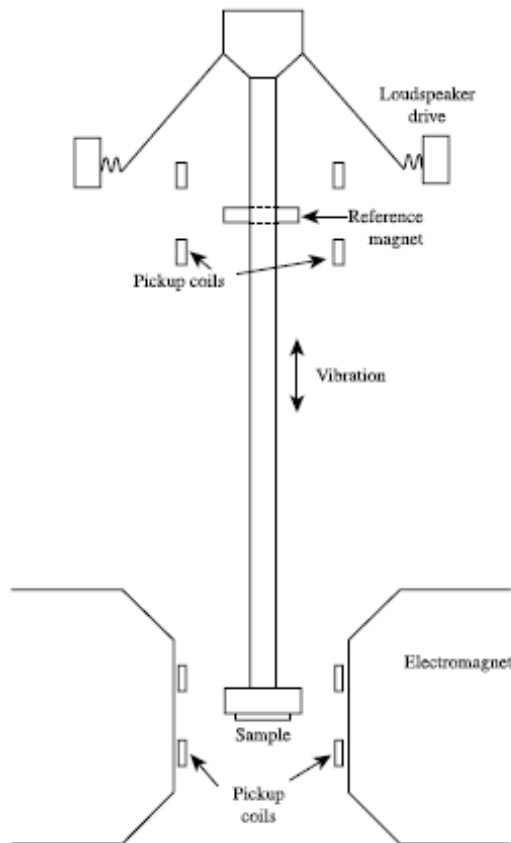
calibration: comparison to a moving Ni sphere



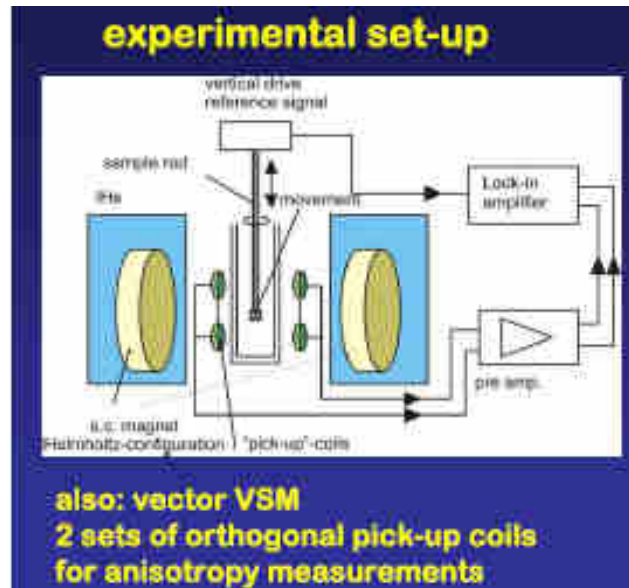
Vibrating sample magnetometer (VSM)

S. Foner, Rev. Sci. Instr 30, 548 (1959)

Schematic

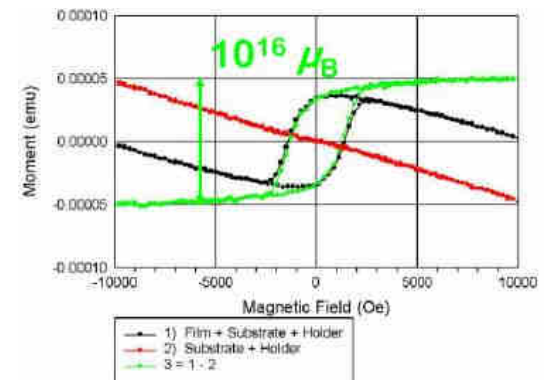


balanced pairs of coils that cancel signals due to variation in the applied field.



The apparatus needs calibration with a specimen of known magnetic moment.

Background needs to be subtracted

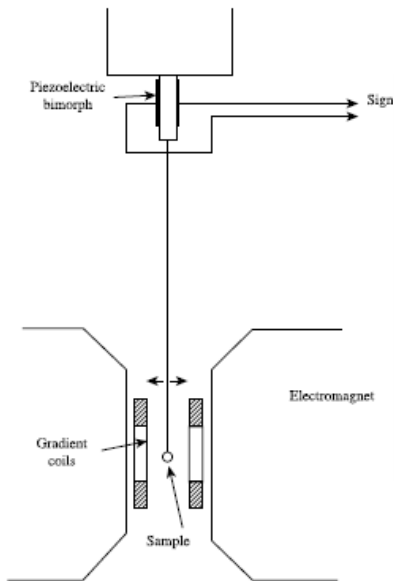


Sensitivity
 $\sim 1 \mu\text{emu} = 10^{14} \mu_B$

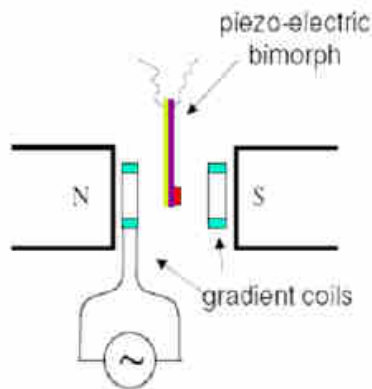


Alternating gradient magnetometry (AGM)

Schematic



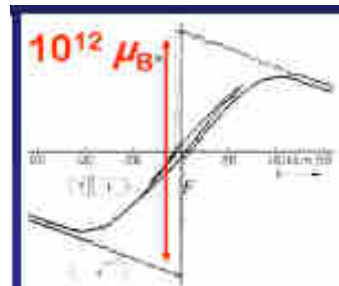
Real tool



force due to a magnetic field gradient

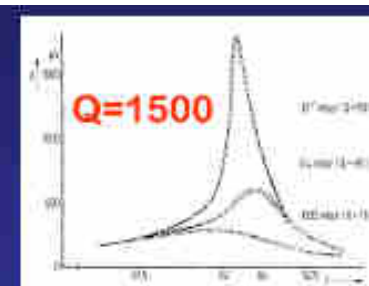
$$F_z = m_z(B_z) \frac{\partial b_z}{\partial z}$$

m : total magnetic moment
 B : magnetizing field
 b : gradient field



diamagnetic moment
of Au superimposed

sensitivity $10^{10} \mu_B$ is possible



resonance gives larger
vibration amplitude

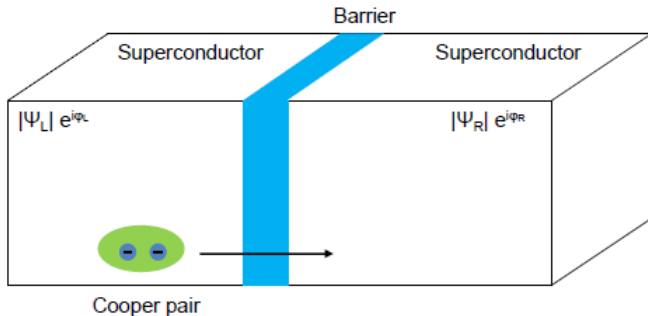
Alternating field gradient, produced by an appropriate coil pair, produces an alternating force on the sample, which causes it to oscillate and flexes the fiber. Frequency of vibration is tuned to a resonant frequency of the system, the vibration amplitude increases by a factor equal to the quality factor Q of the vibrating system. A piezoelectric crystal to generate a voltage proportional to the vibrational amplitude, which in turn is proportional to the sample moment

It is more limited than the VSM in the maximum mass of the sample that can be measured, and tuning the vibration frequency to resonance complicates the measurement. The necessary presence of a field gradient means the sample is never in a completely uniform field, which is sometimes a limitation. Commercial tools sensitivity $\sim 0.1 \mu\text{emu} = 10^{13} \mu_B$



SQUID - principles

Josephson junction



If a (dc) bias current I_b is applied to the JJ

dc Josephson effect

$$I = I_0 \sin(\overbrace{\varphi_L - \varphi_R}^{\delta})$$

I_0 is the maximum supercurrent

$$I_0 < I_c$$

$$I_b > I_0$$

ac Josephson effect

$$\frac{d\delta}{dt} = 2\pi U \Phi_0$$

$$I = I_0 \sin\left(\frac{2\pi U}{\Phi_0} t + \delta_0\right)$$

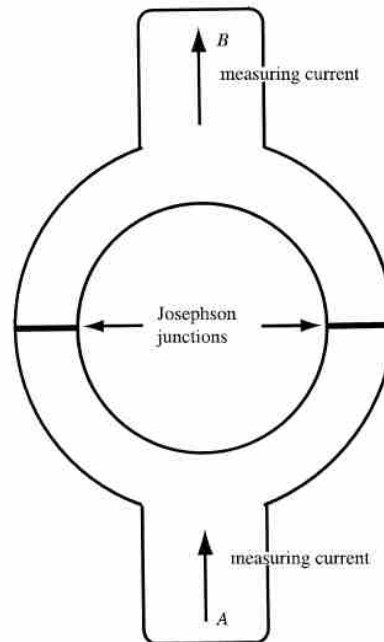
Coupling a very small amount of flux Φ

$$I(\Phi) = I_0 \left| \frac{\sin(\pi \Phi / \Phi_0)}{\pi \Phi / \Phi_0} \right|$$

Fundamental flux quantum

$$\Phi_0 = \frac{h}{2e} \cong 2.00678 \times 10^{-15} \text{ Tm}^2$$

Two Josephson junctions in parallel

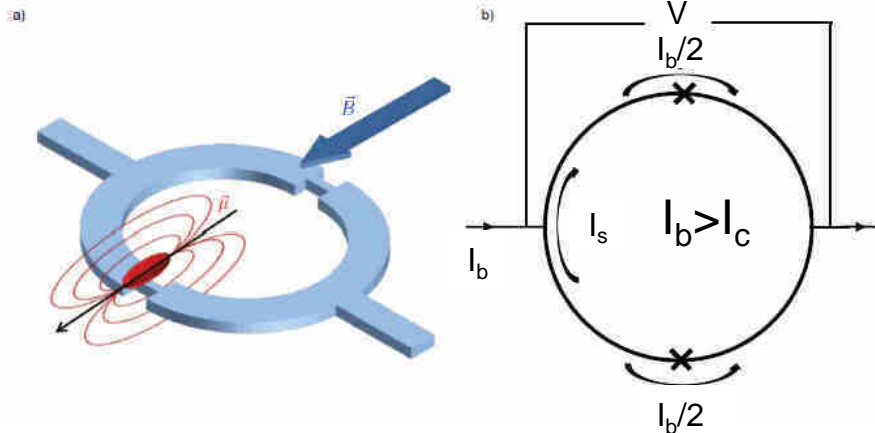


A changing magnetic flux through the ring generates a voltage and a current in the ring, according to Faraday's Law. This induced current adds to the measuring current in one junction, and subtracts in the other. Because of the wave nature of the superconducting current, the result is a periodic appearance of resistance in the superconducting circuit, and the appearance of a voltage between points A and B. Each voltage step corresponds to the passage of a single flux quantum across the boundary of the ring.



SQUID - principles

DC SQUID

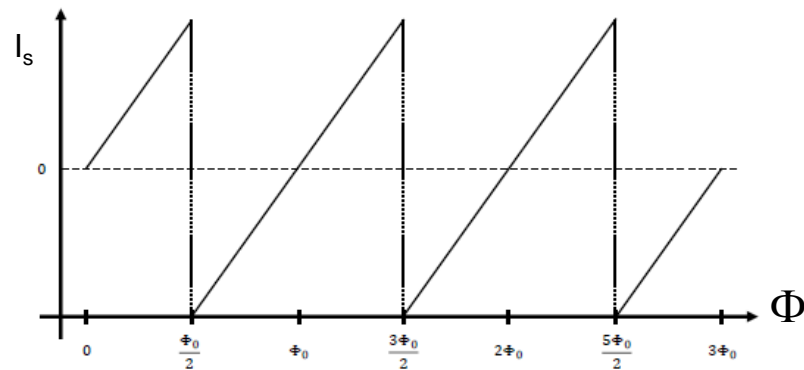


I_s - screening current to effectively cancelling the B flux out in the loop.

A dc SQUID is a device to transform magnetic flux penetrating the loop into voltage currently being the most sensitive device to detect magnetic fields down to the range of 10^{-15} T or respectively changes in magnetic flux on the order of $10^{-8} \Phi_0$.

Fundamental flux quantum

$$\Phi_0 = \frac{h}{2e} \cong 2.00678 \times 10^{-15} \text{ Tm}^2$$



6. | Plot of the screening current I_s over magnetic flux Φ applied to the SQUID.



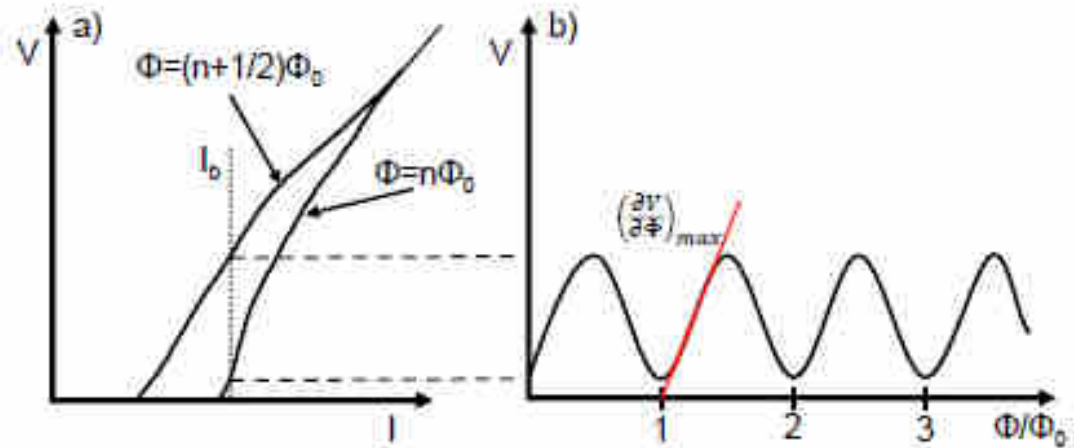
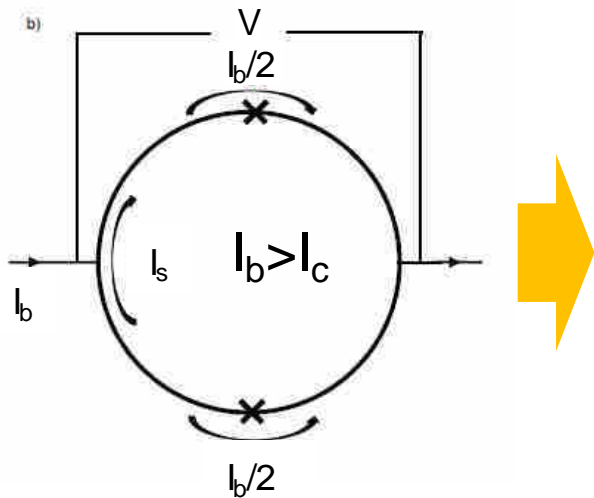
SQUID - principles

Fundamental flux quantum

$$\Phi_0 = \frac{h}{2e} \cong 2.00678 \times 10^{-15} \text{ Tm}^2$$

For increasing applied flux the I-V –curve oscillates between the two depicted extremal curves, leading to a Φ_0 -periodic voltage output of the SQUID.

The obtained sinusoidal V- Φ curve represents the measuring signal of the sensor,

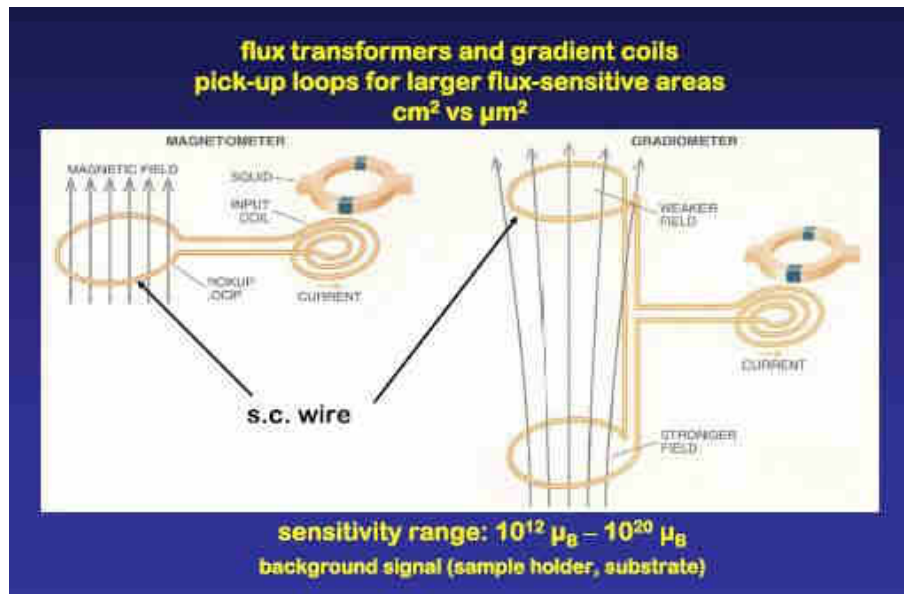


The maximum sensitivity is obtained in the reversal point of the curve where the slope, or transfer function $V_\Phi = dV/d\Phi$ is steepest, as marked in red. To profit from this, SQUIDS can be operated in the flux-locked loop where a feedback flux is generated to maintain the SQUID's working point such that the transfer function is always at a maximum. This way, the sensor is most sensitive and also linear, thus allowing a direct translation of the measured output to flux.

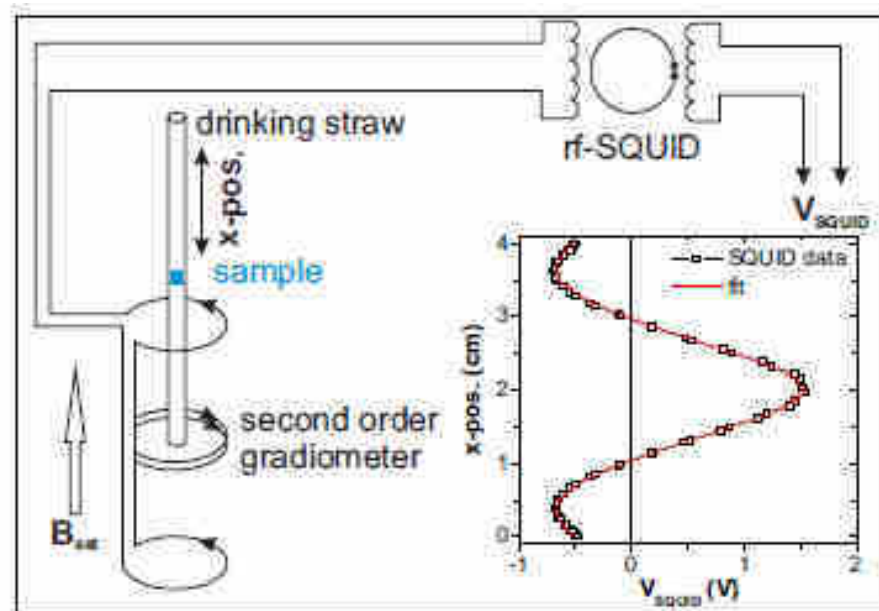


SQUID - magnetometer

Principle



Real tools



Torque magnetometry

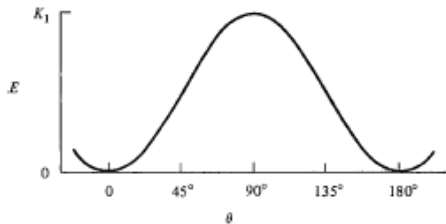
A torque curve is a plot of the torque required to rotate the saturation magnetization away from an easy direction as a function of the angle of rotation.

Sample is placed in a saturating magnetic field. The sample is rotated about an axis through its center, and the torque acting on the disk is measured as a function of the angle of rotation.

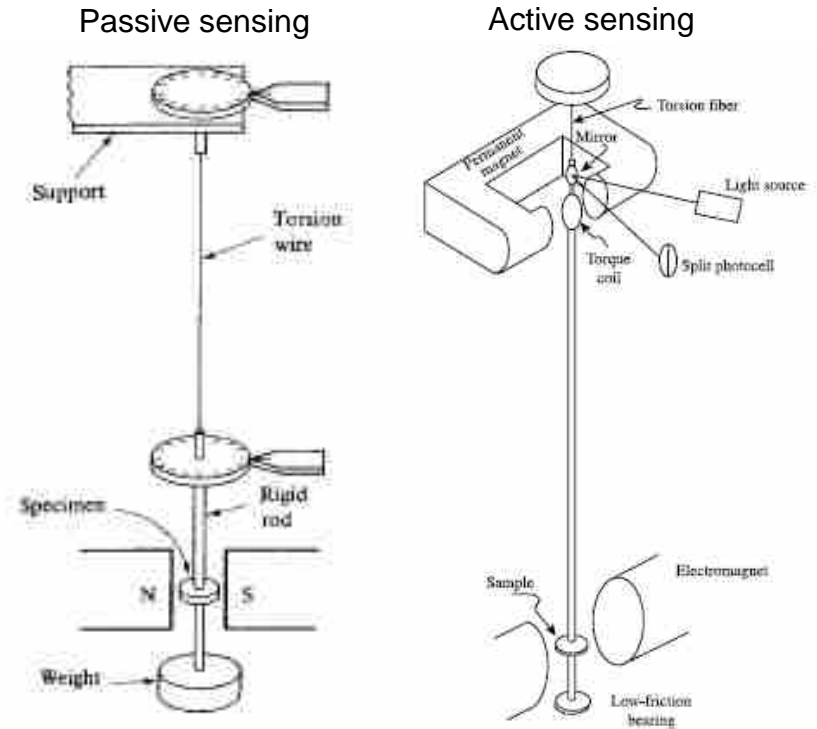
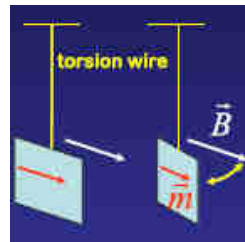
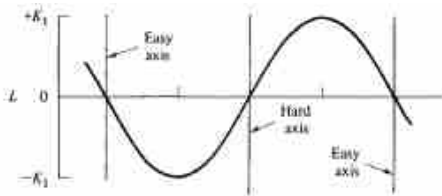
$$\vec{T} = \vec{m} \times \vec{B}$$

$$E_{\text{tot}} = K_1 \sin^2\theta - \mu_0 M_s H \cos\phi = K_1 \sin^2\theta - \mu_0 M_s H$$

Uniaxial anisotropy $E_a = K_1 \sin^2\theta$



Torque $-dE_{\text{tot}}/d\theta = -dE_a/d\theta = -K_1 \sin 2\theta$





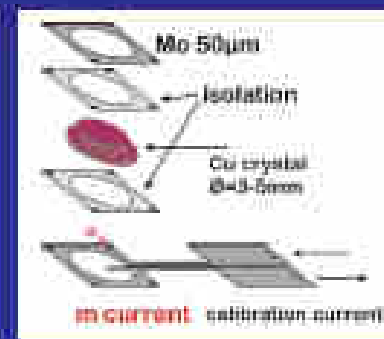
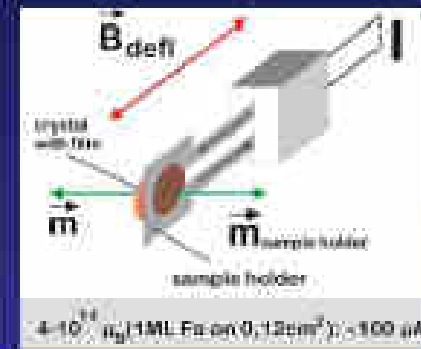
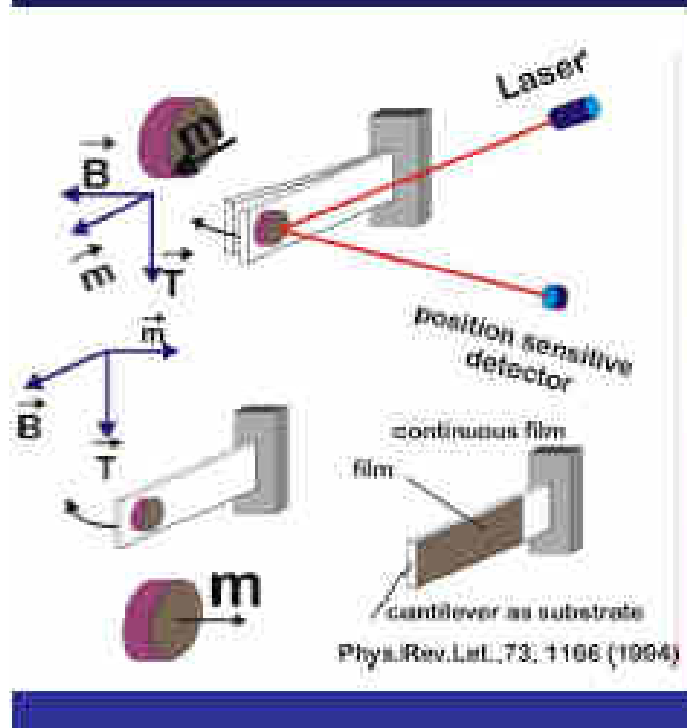
Torque magnetometry

Modern tools (e.g., PPMS)

$$\vec{T} = \vec{m} \times \vec{B}$$

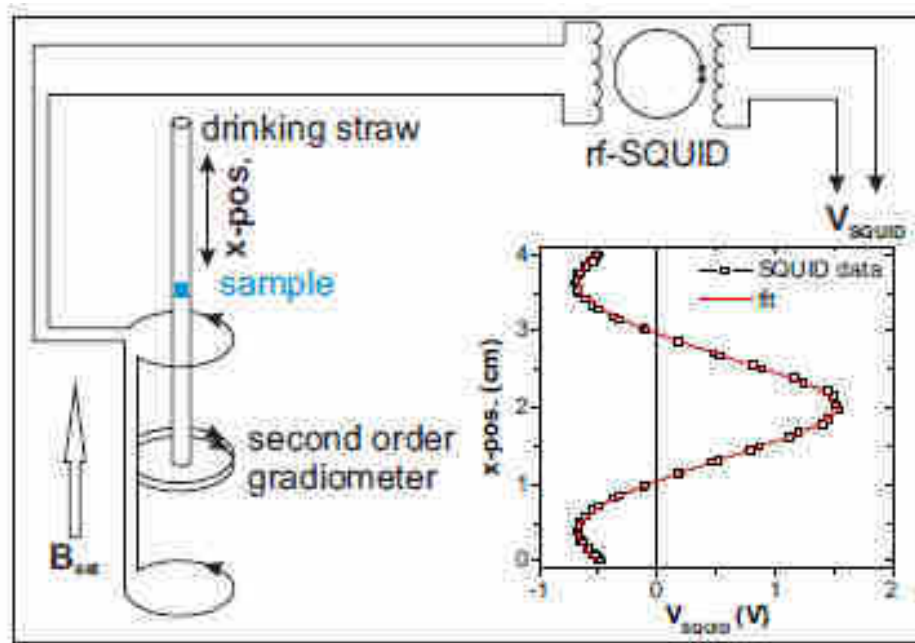
cantilever magnetometry

built-in calibration:





SQUID – magnetometer: limit of detection



SQUID signal is obtained from a fit of the gradiometer signal to a function assuming a point dipole moment either at fixed position

$$V(z) = \mu S [2(r_c^2 + z^2)^{-3/2} - |r_c^2 + (z + \Lambda)^2|^{-3/2} - |r_c^2 + (z - \Lambda)^2|^{-3/2}]$$

- μ magnetic point dipole
- r_c coils radius
- Λ distance outermost coil and central one
- S calibration factor

Asymmetric samples, spatially inhomogeneous, extended....can lead to a break down of the point dipole assumption used in the fit (correction factors).



SQUID – magnetometer: limit of detection

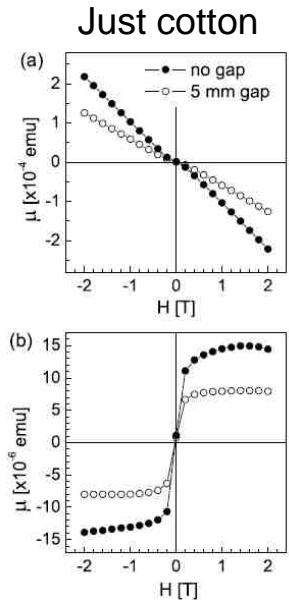
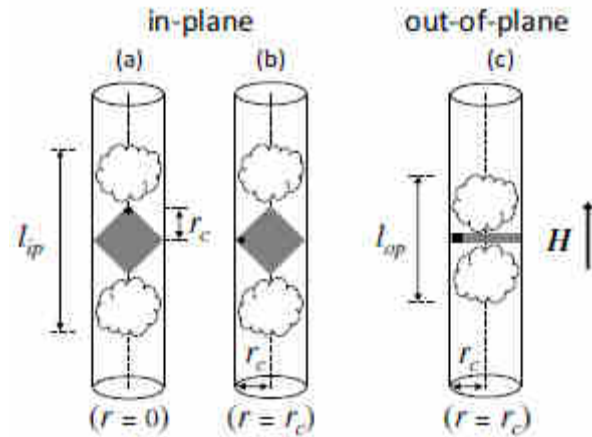
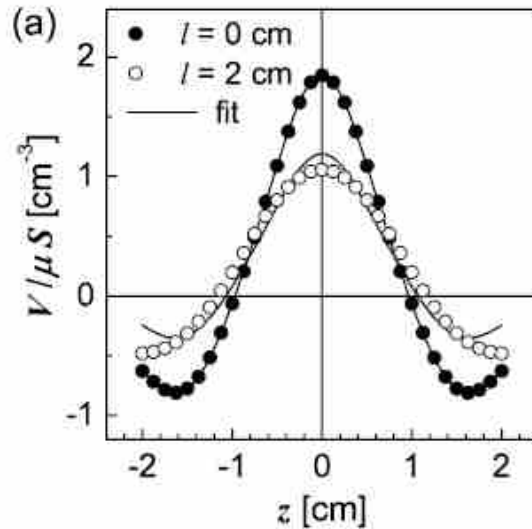
Usually the sensitivity of a SQUID device is of the order of $fT/\sqrt{\text{Hz}}$, which is far below the stray field of a single atomic layer of magnetic material of typical lateral dimensions in the range of few mm^2 . In contrast the sensitivity of commercial SQUID magnetometers is usually provided in emu and typical values are $< 1 \times 10^{-8}$ emu below 250 mT and $< 2 \times 10^{-7}$ emu up to full field (5-9 T).

These specifications usually rely on a measurement with an empty sample holder (straw) and the typical value of artificial signal returned by the fitting routine. It therefore corresponds to the detection sensitivity of the entire pick-up coil detection system including fitting artifacts.

1×10^{-7} emu roughly correspond to the magnetic moment of a single atomic layer of Ni, depending on the chosen specimen size. This translates to a fringing field of the order of nT in a distance of a few mm.



Sample mounting



Example of artefacts due to sample extension.

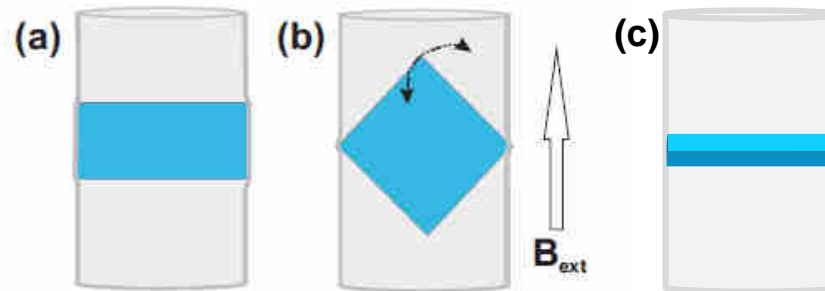
Two limiting cases with equal moment μ : a point-like dipole and a line-like sample with $l = 2$ cm. Figure shows how μ_{exp} decreases with increasing sample length l . Within normal sample sizes (< 5 mm) the effect is negligible ($\sim 4\%$).

However if the ferromagnetic signal is external to the sample, the effects may become significant. In order to fix the position and orientation of a sample inside the measuring straw, it is common to use two small pieces of commercial cotton, which is typically contaminated with small ferromagnetic particles.



Sample mounting

At this level of sensitivity, sample cleanliness and mounting methods become critical!!!



Effects of mounting:

- anisotropies (also contaminats spatial distribution)
- alignment with B_{ext} can be poor, especially for (c) case
- movement of sample
- thermal expansion of holder
- deformations, cuts, marks...

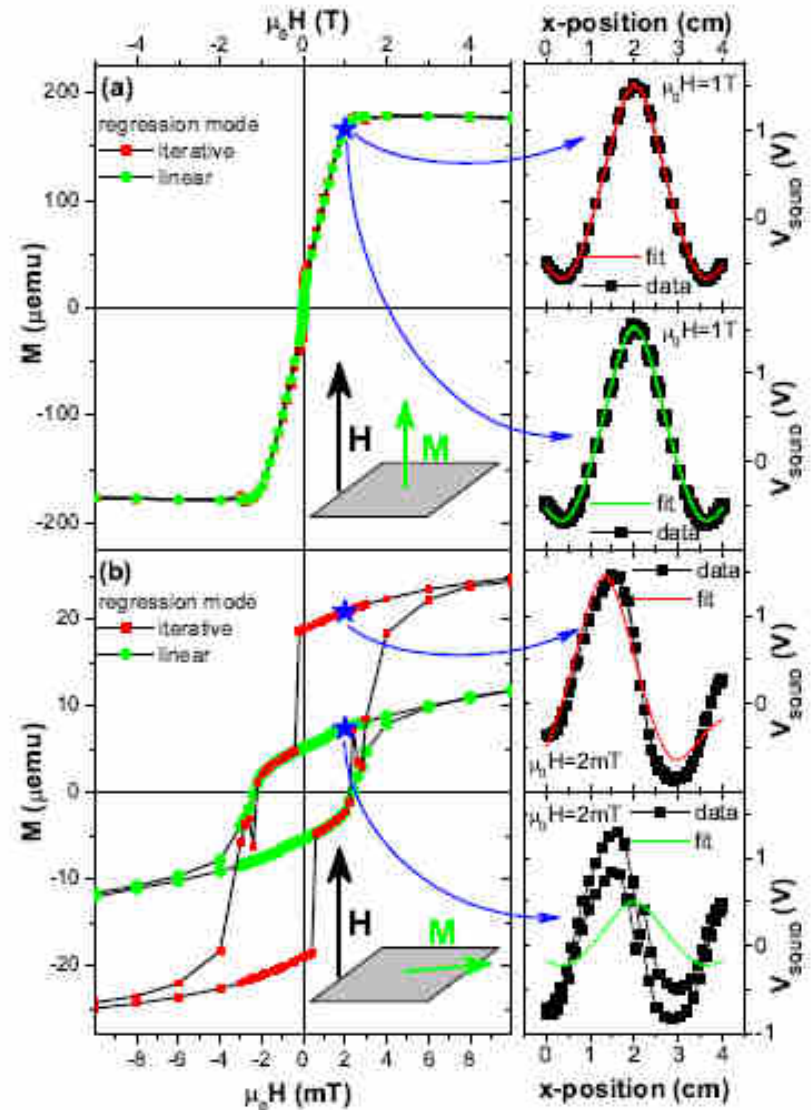
- A. Ney, T. Kammermeier, V. Ney, K. Ollefs, and S. Ye, J. Magn. Mater. 320, 3341–6 (2008)
- L.M.C Pereira et al. J. Phys. D: Appl. Phys. 44, 215001 (2011)



Sample mounting

Artefacts due to non colinearity of M and H , especially affecting hard axis, e.g., polar loops in thin films, in the low field region.

One has to use a better fit for the SQUID voltage signal.





Substrate contribution

For practical magnetometry the specified sensitivity is however not the only relevant quantity to be considered. In many cases in spintronics and magnetism the actual magnetic specimen comes with a substrate or matrix which can be diamagnetic or paramagnetic.

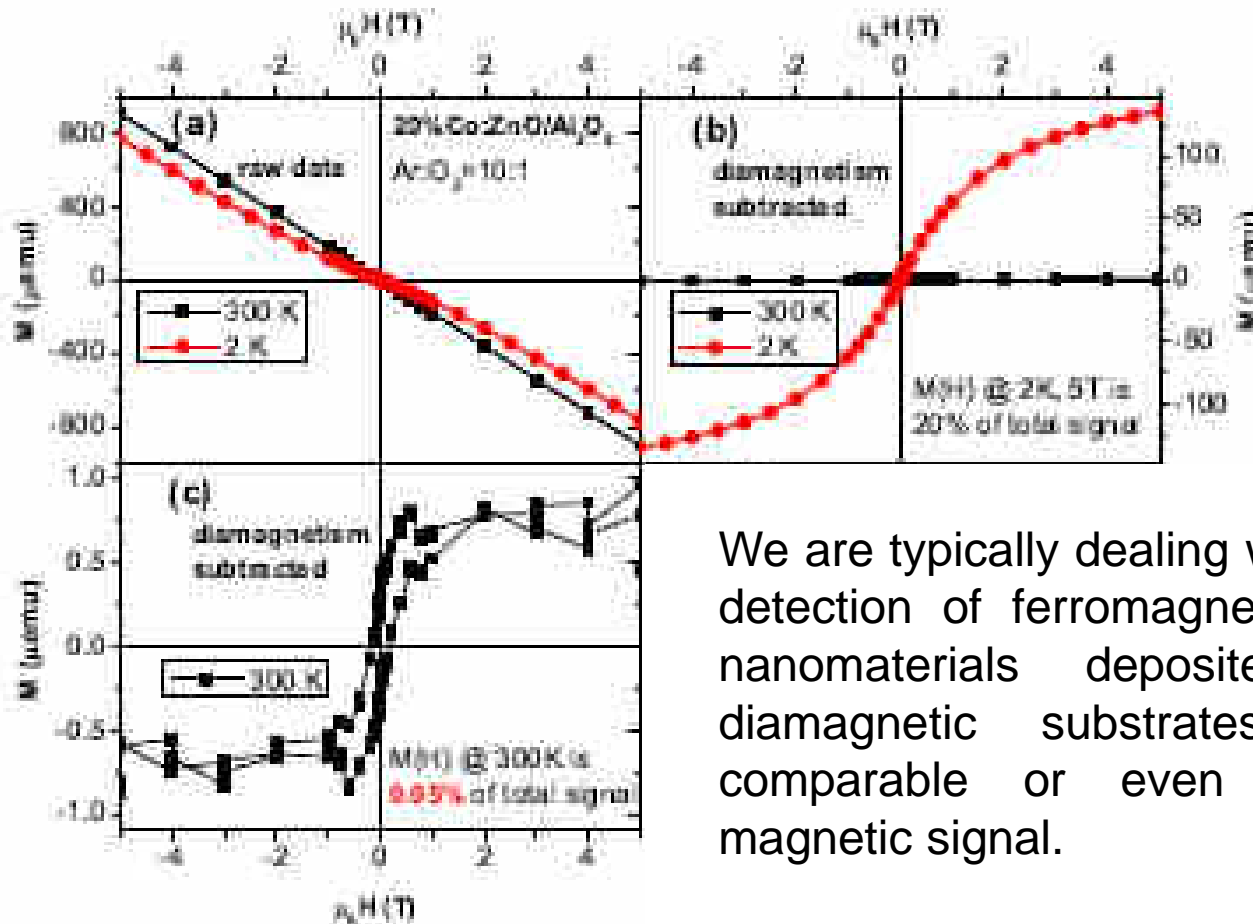
Due to the larger volume of the substrate compared to, e. g., a thin magnetic film already at moderate external magnetic fields the diamagnetic moment of the substrate exceeds the ferromagnetic moment of the film because the diamagnetic moment increases linearly with field while the ferromagnetic moment quickly saturates with fields and stays constant.

Therefore, to derive the magnetic properties of the specimen of interest, one has to subtract a large diamagnetic background from a large measured signal to derive the small magnetic moment of interest.



Substrate contribution

Substrate

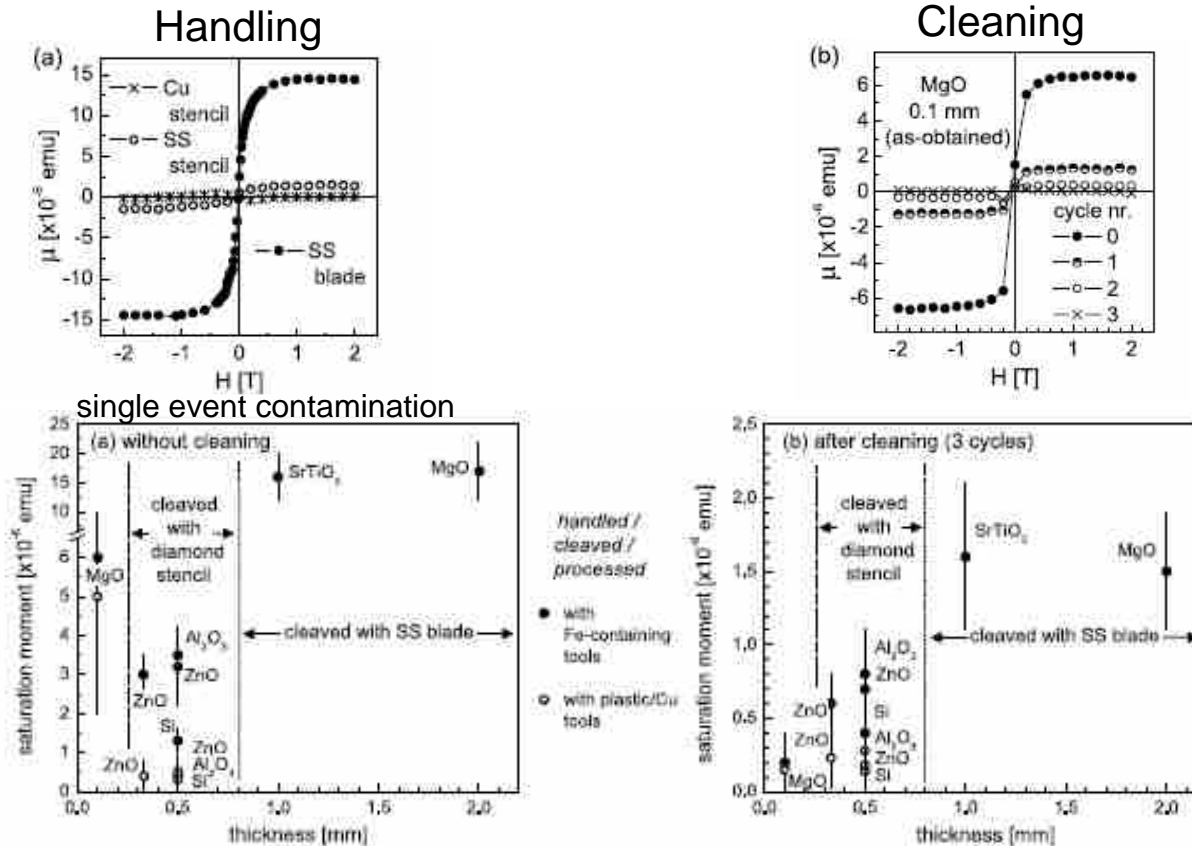


We are typically dealing with the detection of ferromagnetism in nanomaterials deposited on diamagnetic substrates with comparable or even higher magnetic signal.

Substrate signal subtraction is crucial.....well substrate properties are crucial and its volume is huge compared to the actual magnetic material



Substrates contamination



Artefacts associated with magnetic contamination due to sample handling or mounting can be as high as 1×10^{-4} emu.

Whenever Fe-containing tools were used, the level of contamination reached an order of magnitude of 10^{-5} emu.

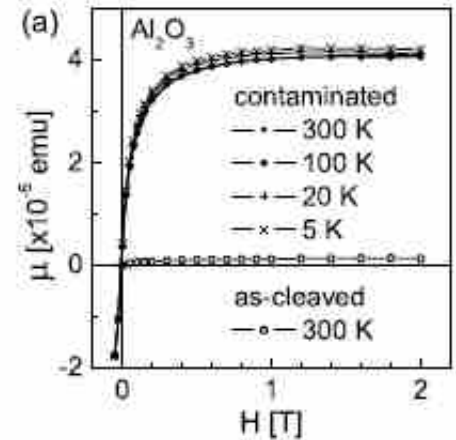
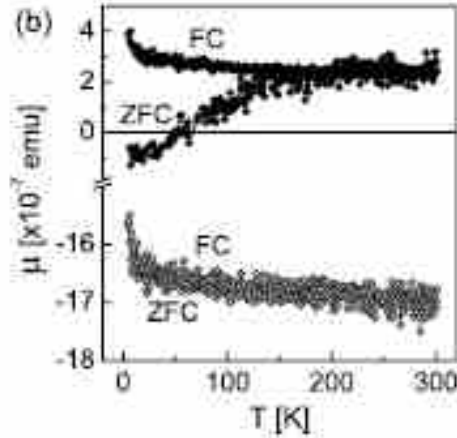
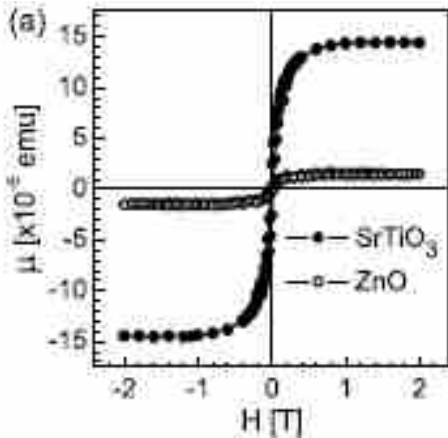
On the other hand, they can be consistently kept below 1×10^{-6} emu using only tools made of non-magnetic materials such as plastic, carbon fibre or copper.

- L.M.C Pereira et al. J. Phys. D: Appl. Phys. 44, 215001 (2011)



Magnetic properties can help?

M-T plots: contaminants are expected to display SPM behavior.....but sometimes they do not!



Diamagnetism is an isotropic property. SPM or ferromagnetic contaminant particles may display some degree of single-particle anisotropy but since they are randomly placed in a sample, their net magnetization should also be isotropic.

Therefore, a diamagnetic substrate, even if contaminated with FM material, is not expected to show anisotropic magnetization with respect to the field direction.

Anisotropy effects could in principle be used as a distinctive feature of intrinsic ferromagnetism.

However, the finite sample size or a non-uniform distribution of the contaminant material can lead to an apparent anisotropy (breaking down of point dipole assumption) when comparing measurements performed with the field parallel (in-plane) and normal (out-of plane) to the sample surface.



Artefacts inherent to SQUID magnetometers

All SQUID magnetometers commonly utilize a superconducting magnet with no direct measurement of the magnetic field at the location of the sample.

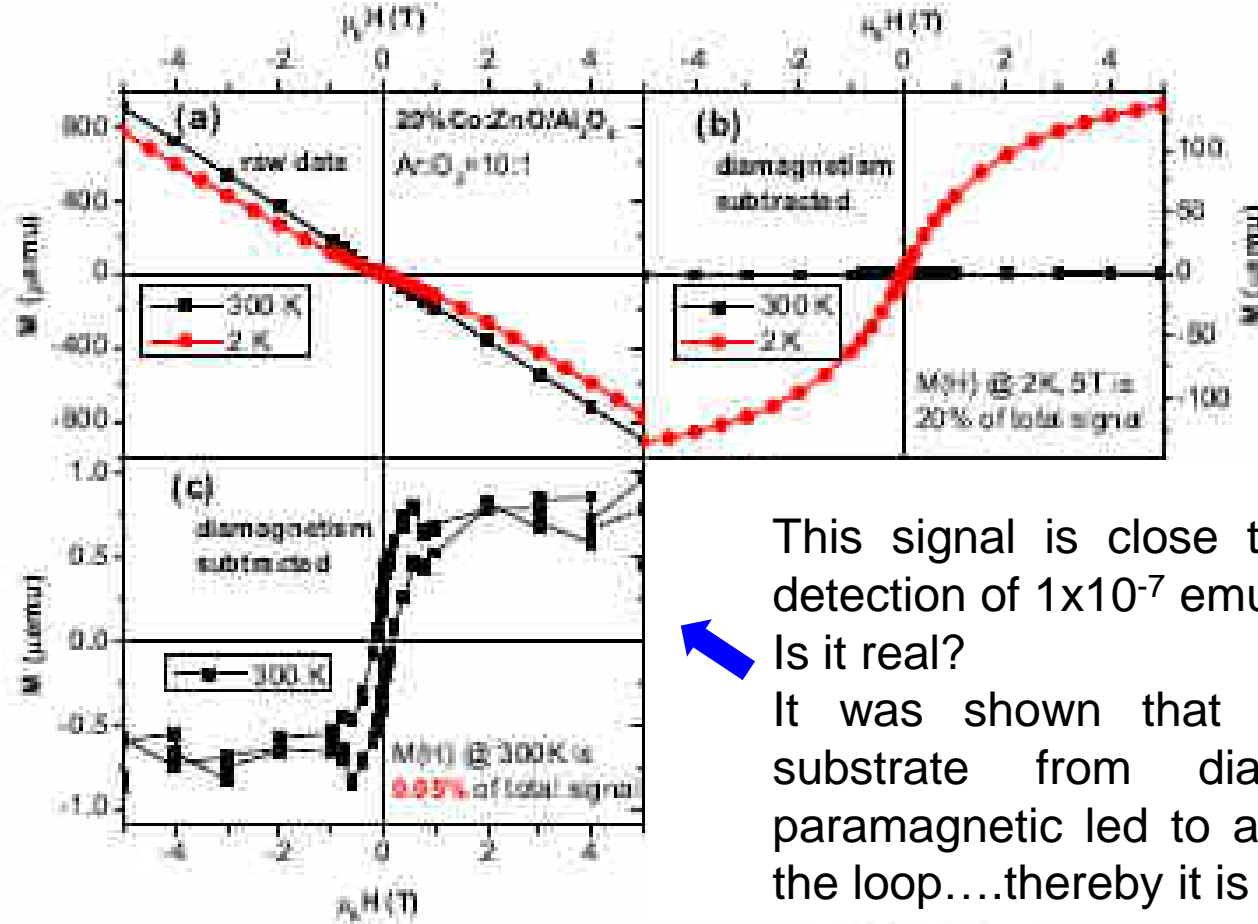
A known issue of all types of superconducting magnets used in these magnetometers is the remanent or trapped field which originates from trapped magnetic flux pinned at defects in the material of the superconducting coil. Most importantly it is directed antiparallel to the last experienced strong field by the magnet.

Recording a magnetization curve up to high magnetic fields, this residual field can neither be avoided nor corrected since the commercial SQUID magnetometers do not measure the magnetic field at the location of the sample. The offset field therefore leads to an apparent residual hysteresis for diamagnetic samples and an inverted hysteresis for paramagnetic samples, which may be held responsible for the possible pitfalls in performing magnetometry using a (usually) diamagnetic substrate, and limits the ultimate detection sensitivity.

The bad part.....is that this artefact shows up as a “ferromagnetic” signal difficult to spot and remove.



Artefacts inherent to SQUID magnetometers



This signal is close to the limit of detection of 1×10^{-7} emu.

Is it real?

It was shown that changing the substrate from diamagnetic to paramagnetic led to an inversion of the loop....thereby it is an artefact.

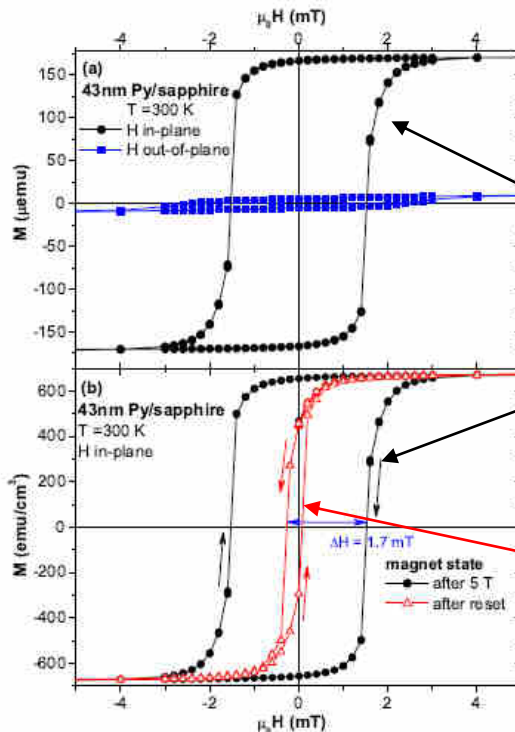
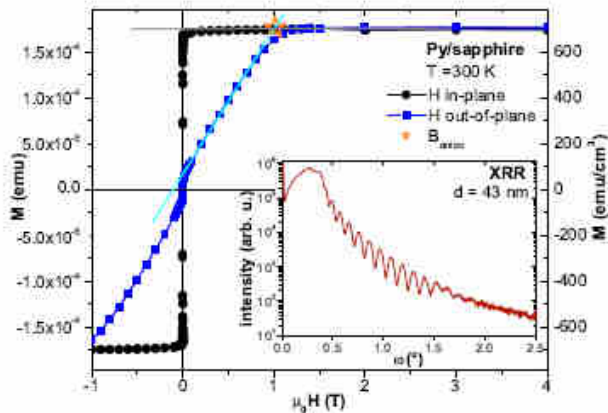
It is actually due to the trapped field: coming from +saturation, it is negative and the signal from the diamagnetic (paramagnetic) substrate results in a positive (negative) moment at nominally "0 field" (at low fields). The opposite coming from -saturation.



Trapped field effect

This is shown clearly in the following example of a 43 nm thick Py film on sapphire, which also demonstrates that this is a potential problem when measuring soft materials with SQUID.

HA loop before an EA one



Inverted loop!!
Negative H_c .

“Real” loop after reset

To measure hard axis loop, we went up to +4 T (-4T) and this left a trapped field of -1.7 mT (+1.7mT) resulting in the observed unphysical behavior. The red-loop was measured after resetting the magnet (heating up above its SC critical temperature and then cooling it down....this consumes helium!!). There is a remaining 0.1 mT shift (bias) which is an instrument unavoidable bias....variable from tool to tool...it is in the specs...not an Exchange bias!!.

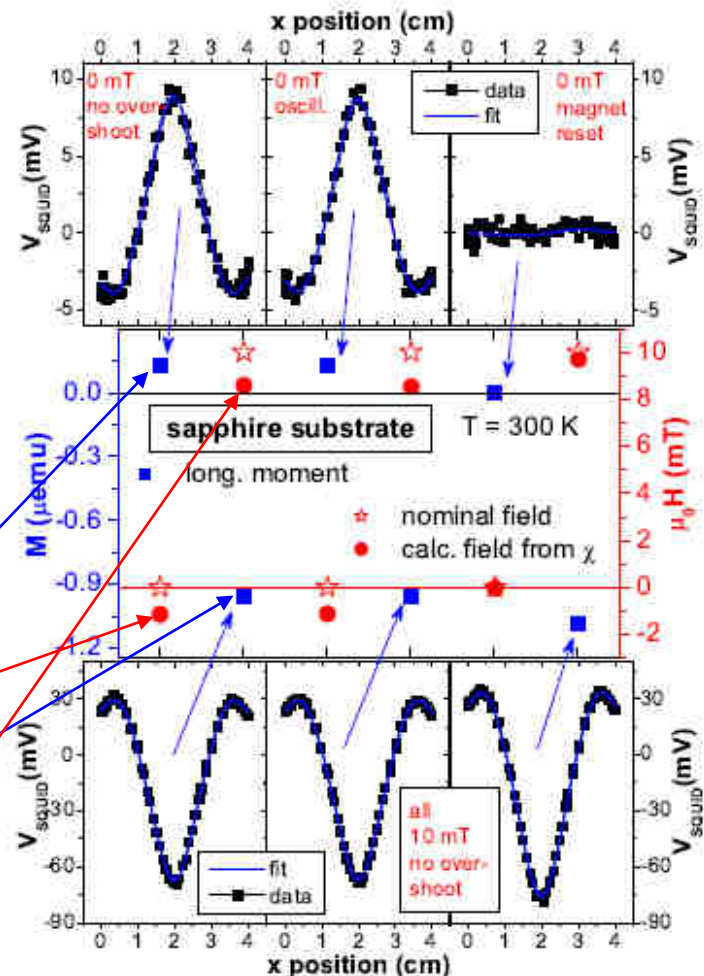


Trapped field characterization

A bare substrate is used and first a standard sequence is recorded (M(H) curve at 300 K). The usual procedure to derive the diamagnetic (in this example) signal of the sample is to take the slope of the high field. A linear fit to the high field data leads to a diamagnetic susceptibility. Since this procedure relies on high-field data above 2 T, small offset fields of the order of 2 mT do not significantly contribute to the uncertainty of the derived value for the susceptibility.

After the standard sequence the magnet has been at 5 T and is now set to nominally 0 mT (open stars). Then a single measurement is performed at nominally zero field which should result in zero magnetization for an ideal diamagnet. small positive magnetization of 1.27×10^{-7} emu is measured (full blue square). From the diamagnetic susceptibility one can calculate that there is a trapped field and how intense (-1.4 mT). Then we set the field to 10 mT and we measure the moment and from the susceptibility we calculate the actual field (8.6 mT) resulting again in a antiparallel (negative) trapped field of 1.4 mT.

Example for a sapphire substrate



A. Ney et al., in press on JAP



Conclusions

- L.M.C Pereira et al. J. Phys. D: Appl. Phys. 44, 215001 (2011)

“We can conclude that the practical limits of SQUID magnetometry for the detection of ferromagnetism in nanomaterials deposited on diamagnetic substrates with comparable magnetic signal, when proper procedures are followed, extrinsic magnetic signals can be reproducibly kept below 5×10^{-7} emu (5×10^{-10} Am², $\sim 10^{13}$ μ_B).

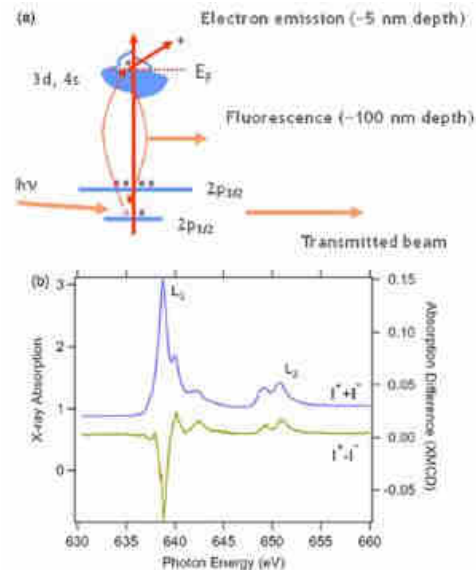
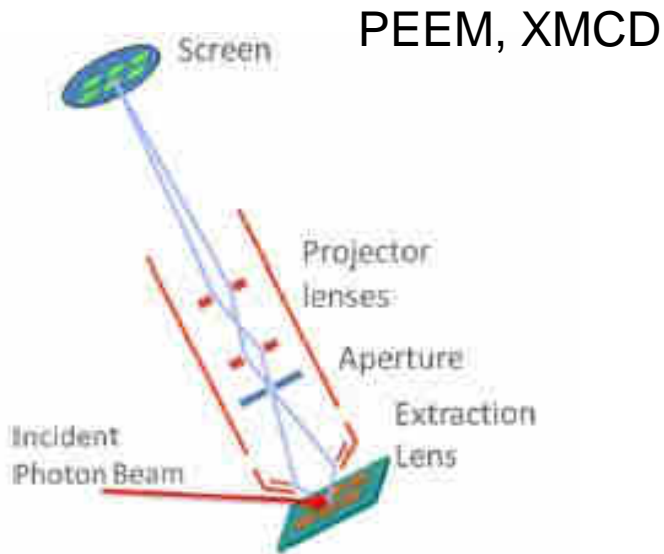
However, the reliability limits should be established independently for the sample processing and handling conditions specific to each experiment, by means of adequate and statistically relevant tests.

We suggest that magnetic behaviour should only be reported reasonably above those limits, as we were unable to identify characteristics of the contaminant magnetism which could be generally used as criteria to distinguish it from intrinsic ferromagnetism.”

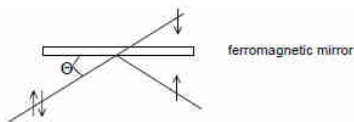


Other techniques... based on large scale facilities.

Synchrotron



PNS



Polarized neutrons source

